This is a repository copy of *Development of β-carotene loaded oil-in-water emulsions using mixed biopolymer–particle–surfactant interfaces*.

White Rose Research Online URL for this paper:
https://eprints.whiterose.ac.uk/181371/

Version: Accepted Version

Development of β-carotene loaded oil-in-water emulsions using mixed biopolymer–particle–surfactant interfaces

Yang Wei[a,b], Dan Zhou[a], Shufang Yang[a], Lei Dai[a], Liang Zhang[a], Like Mao[a], Yanxiang Gao[a]*, Alan Mackie[b]

[a] Beijing Key Laboratory of Functional Food from Plant Resources, College of Food Science & Nutritional Engineering, China Agricultural University, Beijing, P. R. China
[b] Food Colloids and Processing Group, School of Food Science and Nutrition, University of Leeds, Leeds, LS2 9JT, UK

Abstract

In this study, β-carotene loaded oil-in-water emulsions were stabilized by complex interfaces composed of propylene glycol alginate (PGA), rhamnolipids (Rha), and zein colloidal particles (ZCPs). The influence of mixed biopolymer–surfactant, biopolymer–particle, surfactant–particle and biopolymer–surfactant–particle interfaces on the performance of the emulsions was investigated. The stability, microstructure, rheological properties, and *in vitro* gastrointestinal digestion of the emulsions were controlled by regulating the adding sequence and mass ratio of the multiple stabilizers. The droplet size of the emulsion was in the range of 14–77 μm. After encapsulation into the emulsions stabilized by the complex interfaces, the photothermal stability of β-carotene were increased by 41.53% and 21.52%, respectively. The co-existence of particles, biopolymers, and surfactants could induce competitive displacement, multilayer deposition and an interparticle network at the interface. Compared with a single PGA- or Rha-stabilized emulsion, the complex interface-stabilized emulsion reduced the release of FFA by 28.06% and 26.16%, respectively. The interfacial composition of the emulsion and the delayed lipid digestion further affected the bioaccessibility of β-carotene in the gastrointestinal tract (GIT). The mixed biopolymer–particle–surfactant interface-stabilized emulsion could be incorporated in foods, pharmaceuticals and cosmetics for excellent stability, targeted nutrient delivery and controlled lipolysis.
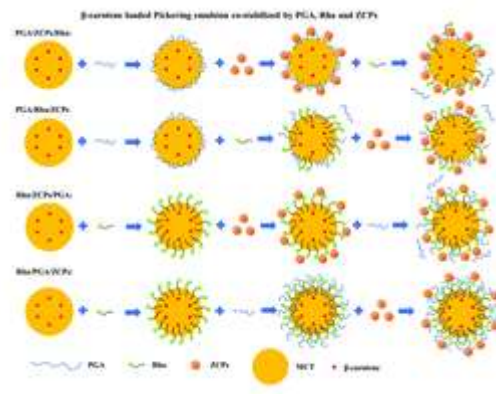
1. Introduction

Oil-in-water (o/w) emulsions stabilized by conventional surfactants and biopolymers have been studied extensively for various practical applications. Surfactants can rapidly occupy the interface and effectively reduce the interfacial tension, which decrease the free energy of the emulsion system (such as phospholipids and saponins).[1] Comparably, the adsorption of biopolymers (proteins and polysaccharides) onto the interface is slower, nevertheless, their adsorption at the interface is more irreversible and provides greater steric repulsion due to their larger molecular weight.[2] Such emulsions

are used in the food and pharmaceutical industry but with limited success due to their poor environmental stability and storage stability against droplet coalescence. Fluctuations in pH and ionic strength usually cause the flocculation of emulsions due to the electrostatic shielding effect. In the human gastrointestinal tract, the presence of exogenous biosurfactants (such as bile salts and phospholipids) may be competitively adsorbed with the original emulsifier onto the interface, which changes the interfacial composition, structure, and stability, thus affecting the rate of lipolysis in the emulsions. For instance, when the originally adsorbed emulsifier is quickly replaced by bile salts, the rate of fat digestion will be increased, which elevates the risk of obesity.[3]

Pickering emulsions stabilized by solid particles have attracted considerable attention due to their potential applications. Compared to traditional emulsions, the adsorption of particles at the interface is usually irreversible owing to their much higher desorption energy.[4,5] Few studies reported that the interaction between nanoparticle and surfactant or biopolymer can stabilize or destabilize emulsions. The stability of emulsions using mixed interfaces is typically observed to be a function of the molecular structure, addition sequence and ratio of emulsifiers and particles.[6,7] Firoozmand, Murray and Dickinson (2009) investigated the behaviour of polystyrene latex and mixed biopolymers (gelatin and oxidized starch) at the interface and reported that non-adsorbed biopolymers caused the depleting flocculation of particles at the interface.[8] The incorporation of particles strengthened the solid-like character with the rise of interfacial elasticity. In another study, the authors improved the water vapor and stability through the addition of zein nanoparticles to the WPI-stabilized films.[9] Xu et al. (2018) prepared emulsions stabilized by alumina nanoparticles and a cationic surfactant (cetyltrimethyl ammonium bromide, CTAB) at very low concentrations with high stability, which further showed that the destabilization of emulsions could be caused by the addition of an oppositely charged surfactant (sodium dodecyl sulfate, SDS), which destroyed the repulsion between the droplets.[10]

Most of the existing studies focused on the influence of emulsifiers on the particle–laden interface. Through adding surfactants or biopolymers to the particle-stabilized interface, they can be co-adsorbed together on the droplet surface due to their amphiphilicity.[11,12] Meanwhile, biopolymers, surfactants, and particles can interact through electrostatic interactions, hydrogen bonding, and hydrophobic forces to form various structures at the interface, such as co-adsorption, complexation, and layer-by-layer deposition.[13–15] The co-stabilization of particles and emulsifiers can reduce the droplet size of particle-stabilized emulsions with less energy input needed, and improve the stability against coalescence by strengthening the electrostatic repulsion and steric hindrance between the droplets or modulating the emulsion viscosity.[16] Nevertheless, the impact of particles on surfactant- or biopolymer-stabilized conventional emulsions is still unclear, especially in the food field. Although recent research investigated the interaction between particle–biopolymer or particle–surfactant binary mixed emulsifiers at the interface,[15,17,18] the influence of complex interfaces consisting of particles, biopolymers and surfactants on the physicochemical properties and gastrointestinal digestion of emulsions has not been studied.

Zein is a distinct amphiphilic plant protein and can be self-assembled into zein colloidal particles (ZCPs) owing to its strong hydrophobicity, with a proportion of over 50% hydrophobic amino acids.[19] Propylene glycol alginate (PGA) is a unique polysaccharide with strong surface activity, which is obtained by the esterification of sodium alginate and different proportions of propylene glycol.[20] Rhamnolipid (Rha) is a microbial surfactant, which is widely utilized to prepare nanoemulsions.[21] It is hypothesized that the interactions among particles, biopolymers, and surfactants, namely ZCPs, PGA, and Rha, can influence the stability and in vitro digestion of oil-in-water emulsions.

The aim of this study was to firstly prepare oil-in-water emulsions in the presence of biopolymers, particles and surfactants, and to explore the effects of the mass ratio and addition sequence of

different stabilizers on the functional attributes of food emulsions. β-Carotene was selected as a model lipophilic nutrient to be incorporated into the emulsions. The structural properties of the emulsions were analyzed through droplet sizing, confocal laser scanning microscopy (CLSM) and cryo-scanning electric microscopy (cryo-SEM). Besides, the rheological properties and stability of the emulsions with different interfacial compositions were tested under various environmental stresses (light, heat, pH and ionic strength). Furthermore, *in vitro* digestion of emulsions was conducted in the gastrointestinal tract (GIT) and the lipolysis and bioaccessibility of β-carotene were determined.

2. Materials and methods

2.1. Materials

Zein (protein content: 91.3%), lipase (pack size: L3126) and bile salts (pack size: 48 305) were purchased from Sigma-Aldrich (USA). It has been reported that lipase activity is 100–500 units per mg protein (using olive oil). The bile salts are composed of 50% deoxycholic acid sodium salt and 50% cholic acid sodium salt. Propylene glycol alginate (PGA) (degree of esterification: 87.9%) was kindly donated by Hanjun Sugar Industry Co. Ltd (Shanghai, China). Curcumin (98%) was purchased from China National Medicine Group Shanghai Corporation (Shanghai, China). Medium-chain triglycerides (MCT, Miglyol 812N) were purchased from Musim Mas (Medan, Indonesia). β-Carotene suspension (30% by mass β-carotene in sunflower oil) was supplied by Xinchang Pharmaceutical Company, Ltd (Xinchang, Zhejiang, China). Rhamnolipid (purity ≥90%) was provided by Parnell Biological Technology Co. Ltd (Shaanxi, China). All other chemical agents were of analytical grade.

2.2. Preparation of particle suspensions, PGA and Rha solutions

In the present study, zein colloidal particles (ZCPs) were prepared by a modified emulsification–evaporation method.[22] Briefly, 4.5 g of zein was dissolved in 450 mL of 70% (v/v) aqueous ethanol solution and stirred at 600 rpm overnight at 25 °C until its complete dissolution. The solution was further homogenized for two cycles at 75 MPa (Niro-Soavi Panda, Parma, Italy). Thereafter, the ethanol in the solution was removed using a rotary evaporator at 45 °C for 25 min and the remaining volume was set to be around 100 mL. The sample was diluted with pH-adjusted water (pH 4.0) to 150 mL. The ZCP suspension was centrifuged (Sigma 3k15, Germany) at 3000 rpm for 10 min to separate large particles and aggregates if any. Finally, the supernatant obtained was adjusted to pH 4.0 using 0.1 M HCl solution. Part of the ZCP suspension was placed at 5 °C for further analysis and the other part was freeze-dried for 72 h to obtain powder samples. Finally, 1.00% (w/v) PGA and Rha solutions were prepared through dissolving 1.0 g of PGA and Rha powder into 100 mL of deionized water overnight at 25 °C and adjusted to pH 4.0 with 1 M HCl.

2.3. Preparation of β-carotene loaded emulsions stabilized by complex interfaces

The β-carotene suspension (20 g) was dissolved in MCT oil (180 g) at 140 °C for 10 s to form the oil phase (3.0 wt% β-carotene).

2.3.1. Method I The primary emulsion was prepared by mixing 7.0 g of PGA (1.0%, w/v) suspension with 15 g of the oil phase at a speed of 18 000 rpm using a blender (Ultra Turrax, model T25, IKA Labortechnik, Staufen, Germany). After the complete dispersion of the oil phase, the mixture was further homogenized for another 5 min. Secondary emulsions were fabricated by mixing the primary emulsion with 2, 4, and 6 g of ZCPs (3.0%, w/v) and homogenized under the same condition. Final emulsions were fabricated by mixed the secondary emulsion with 6, 4, and 2 g of Rha solution (1.0%, w/v), respectively, and homogenized under the same condition, which set the mass ratios of ZCPs to Rha as 2 : 6 (1 : 3), 4 : 4 (1 : 1), and 6 : 2 (3 : 1). The emulsions were termed PGA/2Z6R, PGA/4Z4R, and

PGA/6Z2R according to the mass ratios of ZCPs to Rha. The pH of fresh emulsions was adjusted to 4.0 using 0.5 M HCl. Similarly, when we reversed the order of adding ZCPs and Rha, according to the proportion of Rha and ZCPs, the different emulsions were termed PGA/6R2Z, PGA/4R4Z, and PGA/2R6Z.

2.3.2. Method II The primary emulsion was prepared by homogenizing 7.0 g of Rha (1.0%, w/v) suspension with 15 g of oil phase through the same procedure as aforementioned. Secondary emulsions were fabricated by mixing the primary emulsions with 2, 4, and 6 g of ZCPs (3.0%, w/v) and homogenized under the same condition. Final emulsions were fabricated by mixing the secondary emulsion with 6, 4, and 2 g of PGA solution (1.0%, w/v), respectively, and homogenized under the same condition, enabling the mass ratios of ZCPs to PGA to be $2:6$ ($1:3$), $4:4$ ($1:1$), and $6:2$ ($3:1$). The emulsions were termed Rha/2Z6P, Rha/4Z4P, and Rha/6Z2P according to the mass ratios of ZCPs to PGA. The pH of fresh emulsions was adjusted to 4.0 using 0.5 M HCl. Similarly, when we reversed the order of adding ZCPs and PGA, according to the proportion of PGA and ZCPs, the different emulsions were termed Rha/6P2Z, Rha/4P4Z, and Rha/2P6Z.

2.3.3. Control groups The emulsion was prepared by homogenizing 15.0 g of PGA (1.0%, w/v) or Rha (1.0%, w/v) solution with 15.0 g of the oil phase through the same procedure as aforementioned and termed PGA and Rha.

The primary emulsion was prepared by homogenizing 7.0 g of PGA (1.0%, w/v) suspension with 15 g of oil phase through the same procedure as aforementioned. Secondary emulsions were fabricated by homogenizing the primary emulsion with 8 g of ZCPs (3.0%, w/v) or Rha (1.0%, w/w) solution and termed PGA/ZCPs and PGA/Rha.

The primary emulsion was prepared by homogenizing 7.0 g of Rha (1.0%, w/v) solution with 15 g of oil phase using the same procedure as aforementioned. Secondary emulsions were fabricated by homogenizing the primary emulsion with 8 g of ZCPs (3.0%, w/v) or PGA solution (1.0%, w/v) and termed Rha/ZCPs and Rha/PGA.

2.4. Droplet size and zeta-potential
The droplet size and size distribution were measured after the preparation of emulsions for 12 h with a laser scattering size analyzer (LS230®, Beckman Coulter, USA). The samples were diluted with deionized water until an obscuration rate between 8% and 12% was obtained. The optical properties were evaluated as follows: a refractive index of 1.52 for MCT and absorption of 0.001, and a refractive index of 1.33 for the dispersant (deionized water). The volume-area ($D_{4,3}$) average diameters were calculated using the following equation:

$$D_{4,3} = \frac{\sum n_i d_i^{4}}{\sum n_i d_i^{3}} \tag{1}$$

The n_i is the number of particles with a diameter of d_i.

The zeta-potential of droplets was determined by measuring the direction and velocity of droplet movement in a well-defined electric field using a Zetasizer NanoZS90 (Malvern Instruments, Worcestershire, UK). Emulsions were diluted to a final oil droplet concentration of 0.005 wt% with pH-adjusted deionized water (pH 4.0) to minimize multiple scattering effects. The data were collected from at least 10 sequential readings per sample after 120 s of equilibration and calculated with the instrument using the Smoluchowski model. All the measurements were performed in triplicate.

2.5. Environmental stability

2.5.1. UV radiation The photostability of β-carotene in the emulsions against UV photolysis was tested following a previous study.[16] Briefly, 15 g of fresh samples was placed into a transparent glass vial. Then samples were put into a controlled light cabinet (QSun, Q-Lab Corporation, Ohio, USA) for up to 8 h (35 °C, 0.35 W m^{-2}). The retention rate of β-carotene was plotted against time to calculate the quotient of C_0 and C, where, C_0 is the initial concentration of β-carotene in the fresh emulsions, and C is the remaining concentration of the samples after a period of processing. All experiments were performed in triplicate.

2.5.2. Thermal treatment The emulsions after 12 h storage at ambient temperature (25 °C) were incubated in a water bath (85 °C) for 60 min and then cooled down to 25 °C. The retention rate of β-carotene was detected after thermal treatment.

2.5.3. pH The effect of pH on the emulsion stability was evaluated according to a previous study.18 The designed emulsions after 12 h storage at ambient temperature (25 °C) were adjusted to pH 2.0, 6.0 and 9.0 using either 0.1 M NaOH or 0.1 M HCl.

2.5.4. Ionic strength The emulsions after 12 h storage at ambient temperature (25 °C) were mixed with different weights of NaCl powder for 2 h to assure complete dissolution. NaCl concentrations in different emulsions were adjusted to 10, 50 and 100 mM.[18]

2.6. Confocal laser scanning microscopy (CLSM)
CLSM (Zeiss780, Germany) was used to visualize the interfacial structure of emulsion droplets. The emulsions (1 mL) were stained with a mixed fluorescent dye solution (20 μL) consisting of Nile Blue (0.1%) and Nile red (0.1%) in absolute ethanol for 20 min after vortex oscillation. Then the dyed emulsions were deposited on concave confocal microscope slides and gently covered with a cover slip. Nile Blue was used to stain the ZPNPs and Nile red was applied to dye the oil phase. The CLSM was operated using two laser excitation sources: an argon/krypton laser at 488 nm (Nile red) and a helium neon laser (He–Ne) at 633 nm (Nile Blue).

2.7. Cryo-scanning electron microscopy (Cryo-SEM)
In the Cryo-SEM technique, the sample is vitrified with liquid nitrogen and maintained at a very low temperature, which can preserve the structure of emulsions in a frozen state and allow them to remain stable during the observation.[23] The interfacial structures of the emulsions were observed by Cryo-SEM.[15] The samples were placed on an aluminum platelet, and then transferred to a cryo-preparation system (PP3010T, Quorum Inc., UK) to flash-freeze the samples in liquid nitrogen slush followed by high vacuum sublimation of unbound water. The samples were freeze-fractured in the cryo-preparation chamber, coated with platinum. Then the images were captured using SEM (Helios NanoLab G3 UC, FEI, USA). The analysis was performed at a working distance between 3 and 5 mm with TLD detection at 2 kV.

2.8. *In vitro* digestion, free fatty acid release and β-carotene bioaccessibility
This study used an international standardized in vitro gastrointestinal model with some modifications:[24]

2.8.1. Stomach phase 20 mL of the emulsion was mixed with 20 mL of simulated gastric fluid (SGF) containing 0.0032 g mL^{-1} pepsin to mimic gastric digestion. The pH was adjusted to 2.0 and the sample was then swirled at 150 rpm for 1 h.

2.8.2. Small intestine phase 20 mL of gastric digesta was transferred into a 100 mL glass beaker and then adjusted to pH 7.0. Thereafter, 20 mL of simulated intestinal fluid (SIF) containing 5 mg mL^{-1} bile salt, 0.4 mg mL^{-1} pancreatin and 3.2 mg mL^{-1} lipase was mixed with the digesta in a reaction vessel. The pH was adjusted to 7.0 and the samples were subjected to continuous vibration at 150 rpm for 2 h to mimic small intestine digestion.

The degree of lipolysis was measured through the amount of free fatty acids (FFAs) released. The amount of 0.25 M NaOH required to neutralize the released FFA through lipid digestion was determined using a pH-stat automatic titration unit (Metrohm, Switzerland, 916 Ti-Touch). The amount of FFA released was determined as the percentage of FFA (%) released during the digestion time as described by Li and McClements (2010):[3]

$$\%\text{FFA} = \frac{V_{\text{NaOH}} m_{\text{NaOH}} M_{\text{lipid}}}{2 W_{\text{lipid}}} \times 100\% \tag{2}$$

where $V_{\text{Na}_{\text{OH}}}$ and m_{NaOH} represent the volume (L) and concentration (M) of NaOH solution needed to neutralize the FFA, respectively and W_{lipid} and M_{lipid} represent the initial mass (g) and molecular mass (g mol^{-1}) of the triacylglycerol oil, respectively.

The bioaccessibility of β-carotene was determined after the intestinal digestion.[16] Part of the digesta was processed using a high-speed centrifuge at 15 000 rpm for 60 min at 4 °C. The micelle phase containing the solubilized β-carotene was collected. The content of β-carotene extracted from the initial emulsion and micelle fraction was determined according to the method described in 2.12. The bioaccessibility (%) of β-carotene was calculated using the equation below:

$$\text{Bioaccessibility}\,(\%) = \frac{C_{\text{micelle}}}{C_{\text{initial emulsion}}} \times 100\% \tag{3}$$

where, C_{micelle} and $C_{\text{initial emulsion}}$ are the contents of β-carotene in the micelle fraction and the initial emulsion.

2.9. Statistical analysis

All experiments were performed in triplicate, and the data were expressed as the mean and the standard deviation. The results of all determinations were subjected to one way analysis of variance (ANOVA) using the SPSS 18.0 package (Chicago, USA). Significant differences ($p < 0.05$) of means were determined using Duncan's multiple range test.

3. Results and discussion

3.1. Droplet size

Fig. 1A shows the droplet size of the complex interface-stabilized emulsions using PGA as an inner layer. The droplet size of the PGA-stabilized emulsion was 19.19 ± 0.08 μm. With the incorporation of ZCPs, the droplet size of PGA/ZCPs was elevated to 20.23 ± 0.27 μm. Based on our preliminary results, ZCPs showed a spherical shape with a non-uniform size. The mean size and zeta-potential of ZCPs were 381.1 ± 3.9 nm and 27.43 ± 0.58 mV at pH 4.0, indicating that ZCPs could combine with PGA through

electrostatic attraction at the interface, which provided the extra steric repulsion against the droplet aggregation. The droplet size of PGA/Rha was decreased to 14.89 ± 0.11 μm when PGA and Rha were co-adsorbed onto the droplet surface. The addition of the surfactant decreased the interfacial tension, leading to the rupture of large droplets. The droplet size of the complex interface-stabilized emulsions was dependent on the mass ratio between particles and emulsifiers. At a higher mass ratio between ZCPs and Rha, the droplet size of PGA/6Z2R was increased to 27.23 ± 0.62 μm, which was larger than those of both PGA/ZCPs and PGA/Rha. As reported, PGA and Rha possessed negative charges and ZCPs carried the positive charge at pH 4.0.[25] Therefore, ZCPs and Rha were mainly combined through electrostatic interaction but played an antagonistic role in the stabilization of the emulsions. Rha and ZCPs competitively adsorbed at the interface, causing Rha to squeeze the space where ZCPs was arranged on the droplet surface.[2,26] Meanwhile, ZCPs could restrict the mobility and diffusion of Rha and a small quantity of Rha might induce the bridging flocculation between the droplets.[11,15] With the increase in the Rha level and decrease in the ZCP level, the droplet size of PGA/4Z4R was reduced to 17.67 ± 0.06 μm. Part of Rha might be adsorbed onto the droplet surface through the interfacial gaps between the particles to decrease the interfacial tension. Some of Rha might be adsorbed onto the particle surface to improve the hydrophilicity of particles and reduce the tendency of ZCPs to attract each other.[25]

When Rha was added firstly and then ZCPs, the droplet size of PGA/6R2Z reached the minimum (14.02 ± 0.07 μm) among all the emulsions, which was smaller than that of PGA/2Z6R (18.24 ± 0.04 μm). The results interpreted that even if the mass ratio of ZCPs to Rha remained constant, the different addition sequences of particles and surfactants could affect the interfacial structure. When Rha was added firstly, it could co-adsorb with PGA at the interface and decrease the interfacial tension to stabilize the emulsions.[26,27] When ZCPs were in the outer layer, the particles might restrict Rha from entering the aqueous phase to form micelles, which reduced the depleted effect between the droplets. Therefore, the particle and emulsifier exhibited a synergistic effect on stabilizing the emulsion through electrostatic repulsion and steric hindrance, with the combined advantages of traditional emulsions and Pickering ones. When the Rha content decreased and the ZCP content increased, the size of emulsion droplets was gradually increased. On one hand, the positively charged outer layer of ZCPs neutralized the negative charge carried by PGA and reduced the electrostatic repulsion. On the other hand, the hydrophobic attraction between ZCPs in the outer interfacial layer might cause the droplet aggregation.[18]

Fig. 1B shows the droplet size of the complex interface-stabilized emulsions using Rha as an inner layer. The droplet size of the Rha-stabilized emulsion was 24.08 ± 1.41 μm, which was larger than that of the PGA-stabilized emulsion, indicating that Rha was less efficient to prepare a stable emulsion than PGA without a high energy input. In terms of the emulsions stabilized by the mixed emulsifiers, the droplet size of Rha/ZCPs (76.13 ± 7.06 μm) was much larger than that of Rha/PGA (15.02 ± 0.93 μm). As the molecular dimension of surfactants was smaller than the particles and biopolymers, the adsorption of Rha onto the interface was faster than ZCPs and PGA. Besides, the large molecular dimension limited the penetration of particles and biopolymers through the surfactant-covered interfacial layer to adsorb to the droplet surface. Due to the strong emulsifying ability of PGA and its long-chain structure, it could adsorb to the interface better than ZCPs or complex with Rha. Thereafter, PGA could reduce the interfacial tension and co-stabilize the emulsion along with Rha. On the other hand, ZCPs could be adsorbed to the outer layer of Rha by electrostatic and hydrophobic interactions. Meanwhile, due to the strong attraction between the particles, the particle bridges were easily formed, resulting in droplet aggregation.[28]
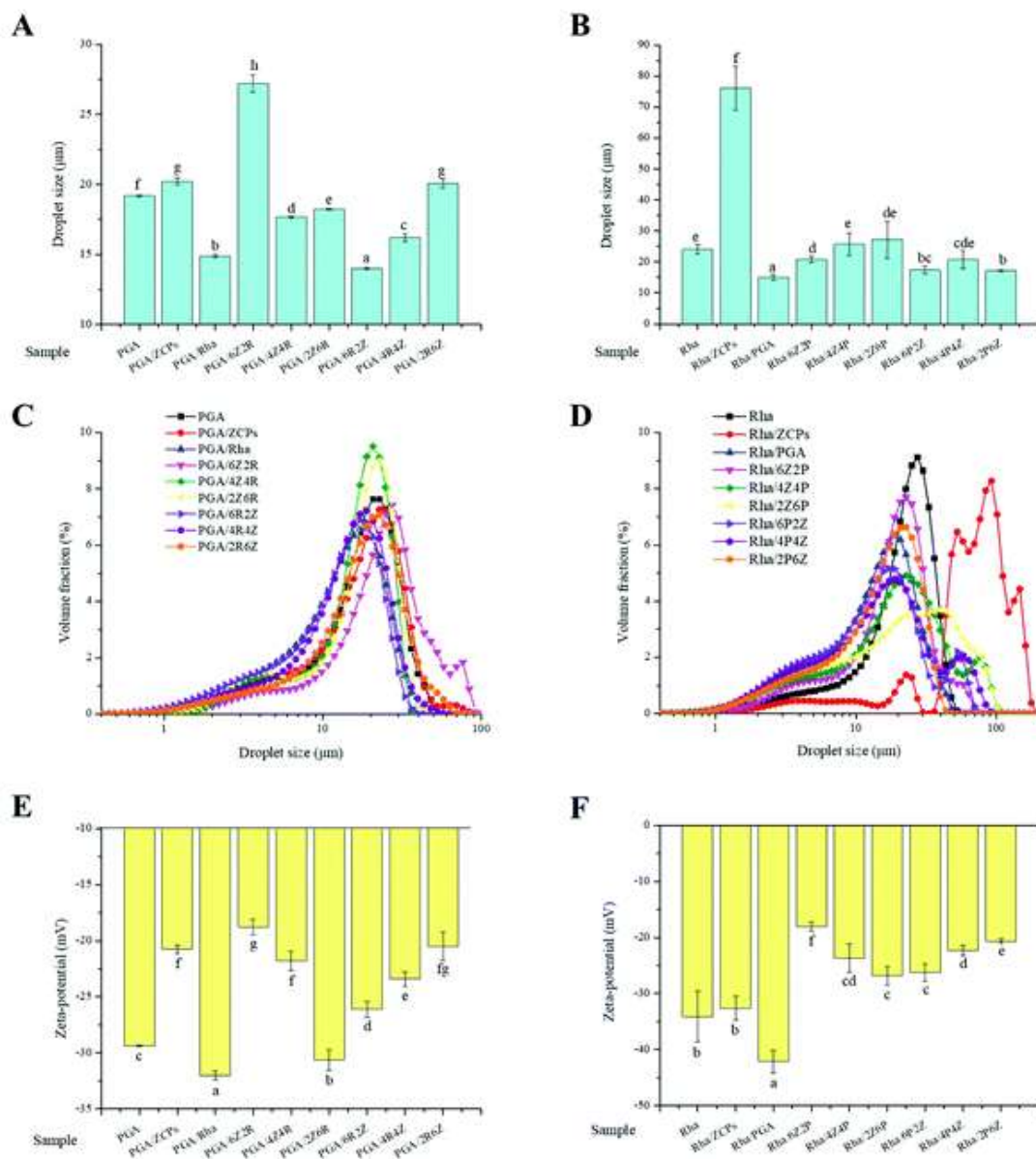
Fig. 1 Mean droplet size, droplet size distribution and zeta-potential of the emulsions stabilized by PGA (A, C and E) or Rha (B, D and F) as an inner layer (different superscript letters (a, b, c…) in the figure indicate significant differences ($p < 0.05$)).

The droplet size of the emulsions with Rha as an inner layer was larger than that of Rha/PGA, but smaller than that of Rha/ZCPs (Fig. 1B). This result indicated that the particles hardly showed a strong emulsifying ability at the interface, but they could increase the thickness of the interface layer due to the rigid structure. When PGA was adsorbed on the outer layer, it could reduce the aggregation between the droplets induced by the particle bridges. With the rise in the PGA level and decrease in the ZCP level, the droplet size was elevated from 20.69 ± 1.04 μm (PGA/6Z2P) to 27.22 ± 5.95 μm (PGA/2Z6P). This phenomenon might be explained by that excessive PGA entered into the aqueous phase and induced the depletion flocculation between the droplets.[18] When PGA was added firstly and then ZCPs, the droplet size of the emulsions remained stable with the mass ratio between PGA and ZCPs varying.

The droplet size distribution of the complex interface-stabilized emulsions was demonstrated (Fig. 1C). It was observed that almost all the emulsions showed a monomodal distribution except for PGA/6Z2R, which had a small peak around 70 μm. A small quantity of Rha could cause the bridging flocculation of the droplets in the outer layer of the interface.[15] Fig. 1D shows the droplet size distribution of the emulsions with Rha as an inner layer. It could be observed that the most severe aggregation of droplets occurred in Rha/ZCPs, which was consistent with its largest mean size. Apparently, the particles in the outer layer caused the aggregation and bridging between the droplets due to their strong hydrophobicity. Additionally, the partial aggregation of droplets occurred in Rha/4Z4P and Rha/2Z6P, which was mainly caused by the depletion effect of excessive PGA in the continuous phase.[16,28]

3.2. Zeta-potential

As shown in Fig. 1E, the zeta-potential of the emulsions with PGA as an inner layer was demonstrated. The zeta-potential of the PGA-stabilized emulsion was −29.37 ± 0.05 mV. With the incorporation of ZCPs, the zeta-potential of PGA/ZCPs was reduced to −20.76 ± 0.37 mV because ZCPs carried a positive electrical charge at pH 4.0. Nevertheless, the zeta-potential of PGA/Rha was slightly reduced to −32.03 ± 0.42 mV with the addition of Rha. In the presence of ZCPs, PGA, and Rha, the zeta-potential of the complex interface-stabilized emulsions was dependent on the mass ratio between ZCPs and Rha. The higher level of Rha and lower level of ZCPs formed droplets with a more negative charge and vice versa. Fig. 1F shows the zeta-potential of the emulsions with Rha as an inner layer. The zeta-potential of the Rha-stabilized emulsion was −34.10 ± 4.52 mV, which was decreased to −42.13 ± 2.00 mV (Rha/PGA) with the complexation with PGA. When the particles were added firstly in the presence of a high proportion of ZCPs, the zeta-potential of Rha/6Z2P was reduced to −18.03 ± 0.81 mV. With the increase in the PGA content, the negative charge of the emulsions was gradually increased, which was similar to the emulsions as PGA was added firstly and then ZCPs. The results were consistent with our previous study.[18]

3.3. Physicochemical stability under different environmental stresses

3.3.1. Physical stability The influence of the interfacial composition on the physical stability of the complex interface-stabilized emulsions was investigated through imposing centrifugal force. PGA and PGA/ZCPs exhibited a better physical stability than other emulsions in the control group (Fig. 2A). As an anionic polysaccharide, PGA provided sufficient spatial and electrostatic repulsion between the droplets. With the incorporation of ZCPs, the electrostatic repulsion was slightly reduced owing to the charge neutralization. However, the enhanced steric repulsion could effectively prevent the droplet coalescence in the presence of particles. Comparably, the stability of Rha and Rha/ZCPs became much worse than that of PGA and PGA/ZCPs. Although the surfactant could adsorb to the interface more quickly and reduce the interfacial tension, it could not prevent coalescence during centrifugation without sufficient steric hindrance.[1] When Rha and PGA co-adsorbed at the interface, Rha/PGA became more stable than PGA/Rha. As PGA lied in the outer layer, Rha/PGA provided a better steric repulsion against droplet coalescence. Moreover, it might restrict the competitive displacement between Rha and PGA at the interface. Comparably, Rha might penetrate into the PGA-covered interface due to its smaller molecular size, which was prone to cause the interface film to rupture.[2]
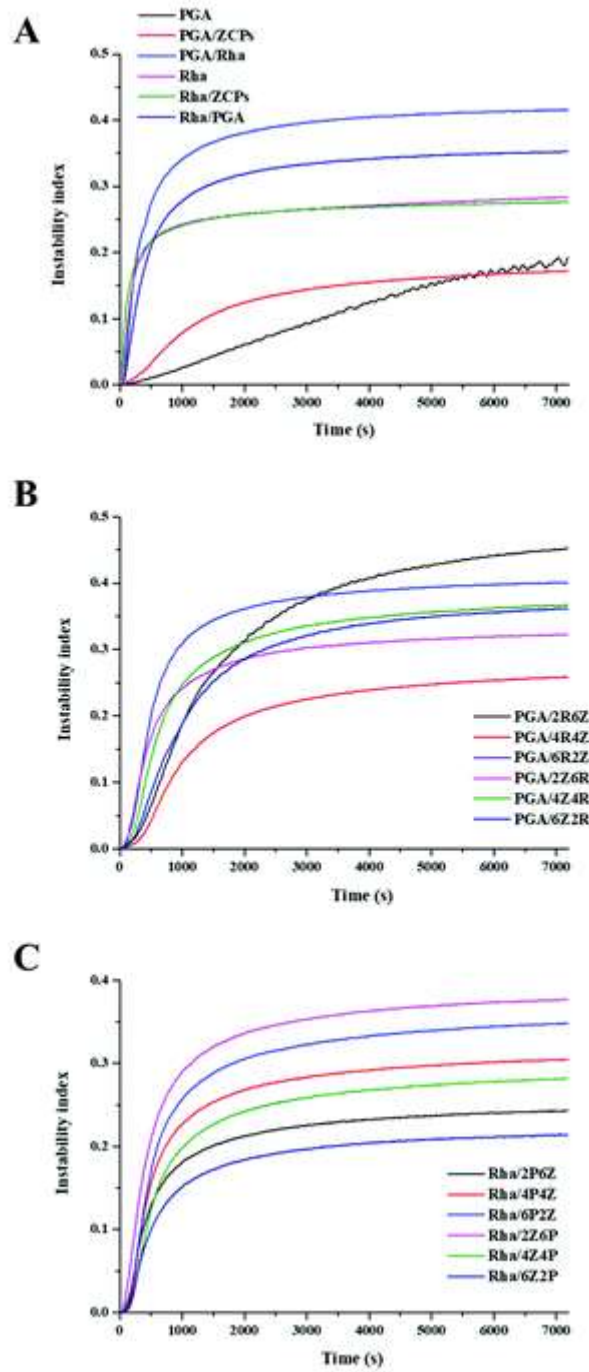
Fig. 2 Physical stability of the emulsions stabilized by PGA, PGA/ZCPs, PGA/Rha, Rha, Rha/ZCPs, and Rha/PGA (A); physical stability of the emulsions using PGA as an inner layer (B) and Rha as an inner layer (C).

Fig. 2B shows the physical stability of the emulsions using the complex interfaces with PGA as an inner layer. When Rha was added firstly and then ZCPs, PGA/4R4Z was the most stable among all the emulsions. The increased ZCP level enhanced the instability index. The outer particles might induce bridging between the droplets and result in droplet aggregation. The higher Rha content made PGA/6R2Z unstable due to the competitive displacement between PGA and Rha at the interface. Meanwhile, the reduced particle level could weaken the steric repulsion between the droplets. When

ZCPs were added firstly to the PGA-covered interface and then Rha, the mass ratio of ZCPs to Rha showed an insignificant impact on the emulsion stability.

The physical stability of the emulsions stabilized by the complex interface using Rha as an inner layer is depicted in Fig. 2C. When PGA was added firstly to the Rha-stabilized interface and then ZCPs, the stability of the emulsions improved with the increase in the particle level. A similar phenomenon was observed in the stability of the emulsions with PGA as an outer layer, which was increased at a lower level of PGA. However, the emulsions with ZCPs as an outer layer became more stable at a higher level of PGA. Rha/6Z2P exhibited the best physical stability among all the emulsions. These results could be ascribed to two aspects: firstly, the presence of particles indeed enhanced the emulsion stability through providing steric repulsion, but the particles anchored at the outer layer of the interface could cause bridging flocculation between the droplets at a higher level.[28] Secondly, PGA in the outer layer restricted the particle bridges between the droplets, nevertheless, excess PGA might enter into the aqueous phase and induce depletion flocculation.[16]

3.3.2. Photostability Among the emulsions with PGA as an inner layer, β-carotene entrapped in the PGA-stabilized emulsion degraded most quickly (Fig. 3A), with 51.12% of β-carotene remaining after 8 h of UV radiation. The photostability of β-carotene was improved slightly with the incorporation of Rha or ZCPs into the PGA-covered interface, which was further enhanced when PGA, ZCPs, and Rha co-existed at the interface. These results demonstrated that ZCPs and Rha showed a synergistic effect on protecting β-carotene in the emulsions with PGA as an inner layer, and the complex interfaces provided a better protection for the emulsions with a thicker interface to reduce light transmission. It was observed that β-carotene showed the highest retention rate (72.35 ± 1.66%) in PGA/2Z6R, which was increased by 41.53% compared to that of the PGA-stabilized emulsion. Generally, unlike the physical stability, the emulsions with Rha as an outer layer showed a better photostability of β-carotene compared to that of the emulsions using ZCPs as an outer layer. When Rha was added to the particle–laden interface, it could fill the gaps between the particles and therefore limit the transit of light.[15] Nevertheless, the competitive displacement between PGA and Rha could occur at the interface when Rha was added firstly to the PGA-covered interface, which reduced the emulsion stability.[2,27]

The Rha-stabilized emulsion exhibited a higher retention rate of β-carotene (73.25 ± 0.17%) than the PGA-stabilized one (Fig. 3B). The larger droplet size of the Rha-stabilized emulsion resulted in a smaller surface area, reducing the exposure of light. However, the photostability of β-carotene in the Rha-stabilized emulsion was decreased with the addition of ZCPs or PGA due to their poor physical stability (Fig. 2A). When ZCPs or PGA were used as the outer layer of the interface, excess particles and biopolymer might cause the bridging or depletion flocculation between the droplets, respectively.[28,29]

Among all the emulsions using Rha as an inner layer, Rha/2Z6P exhibited the highest retention rate of β-carotene (84.54 ± 1.05%) after 8 h of UV light treatment, which was enhanced by 15.41% compared to the Rha-stabilized emulsion. Compared with recent studies, the emulsions with complex interfaces in this study showed the equivalent or better protection of β-carotene entrapped. In our previous study, the particles and lactoferrin were used to co-stabilize a Pickering emulsion and β-carotene entrapped remained around 80% after 4 h light treatment, which was elevated above 90% using biopolymer–surfactant–particle complex interfaces.[16] In another study, Liu et al. (2016) reported that 70% of β-carotene remained in the emulsion stabilized by chlorogenic acid–lactoferrin–polydextrose conjugates after 8 h of UV radiation.[30] Different stabilizers (ZCPs, PGA, and Rha) exerted a synergistic effect on protecting β-carotene from chemical degradation, which might form a thicker interfacial layer to restrict the penetration of light and affect the diffusion of oxygen, free radicals, and prooxidants at the interface than any single emulsifier.[31]
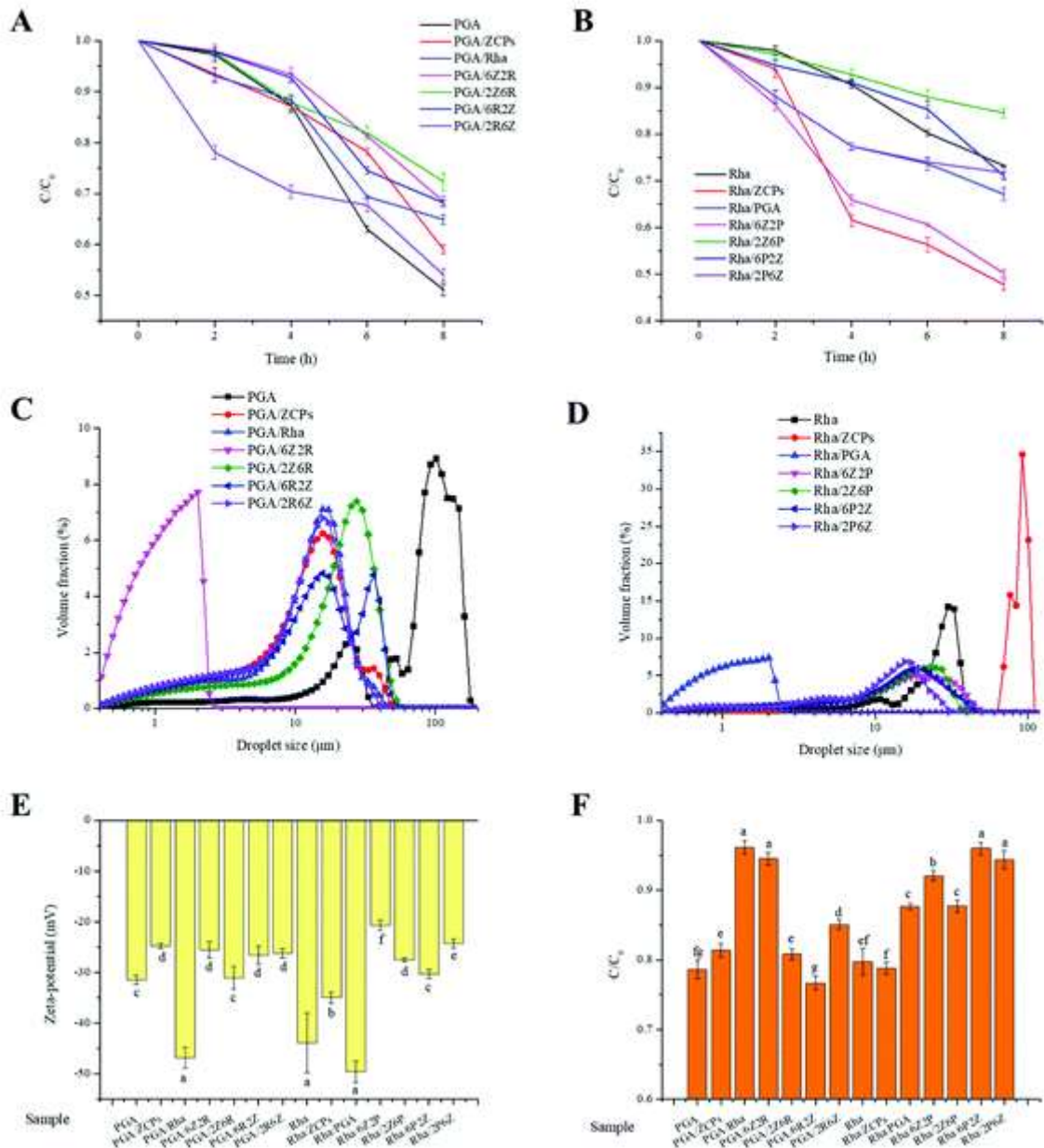
Fig. 3 Photostability of β-carotene entrapped in the emulsions using PGA (A) or Rha (B) as an inner layer; influence of heating on the droplet size distribution of the emulsions using PGA (C) or Rha (D) as an inner layer; influence of heating on the zeta-potential of the emulsions (E); thermal stability of β-carotene entrapped in the emulsions (F) (different superscript letters (a, b, c…) in the figure indicate significant differences ($p < 0.05$)).

3.3.3. Thermal stability The droplet size of the PGA-stabilized emulsion was elevated from 19.19 ± 0.08 to 87.20 ± 0.87 μm after thermal treatment (Table 1), indicating that PGA was incapable of preventing droplet aggregation alone. With the incorporation of ZCPs and Rha, the thermal stability of the emulsions stabilized by the complex interface was improved. The droplet size of the emulsions remained constant, mainly because the particles existing in the interfacial layer provided steric repulsion to prevent the droplets from coalescing.[5,32] A similar phenomenon was observed in the emulsions with Rha as an inner layer. The droplet size of the Rha-stabilized emulsion was increased from 24.08 ± 1.41 to 30.80 ± 2.05 μm, indicating that Rha could scarcely stabilize the emulsion solely

against aggregation during thermal treatment. With the adsorption of ZCPs, the droplet size of Rha/ZCPs was increased from 76.13 ± 7.06 to 86.46 ± 1.30 μm, which interpreted that the particle bridges might be formed due to the strong hydrophobic attraction promoted by heating. Comparably, with the combination of surfactant and biopolymer, Rha/ZCPs remained more stable with a constant droplet size. Additionally, all the emulsions stabilized by the complex interfaces consisting of Rha, ZCPs, and PGA exhibited a consistent droplet size.

Table 1 Mean droplet size of different oil-in-water emulsions stabilized by a single emulsifier and complex interface

| Emulsion | $D_{4,3}$ (μm) | | | |
	Original emulsion	After heating	Stomach	Small intestine
PGA	19.19 ± 0.08[def]	87.20 ± 0.87[a]	20.24 ± 0.15[efg]	1.94 ± 0.08[c]
PGA/ZCPs	20.23 ± 0.27[cde]	13.19 ± 0.33[jk]	30.09 ± 0.36[c]	2.52 ± 0.14[b]
PGA/Rha	14.89 ± 0.11[ef]	12.85 ± 0.75[k]	13.38 ± 0.08[h]	2.49 ± 0.12[b]
PGA/6Z2R	27.23 ± 0.62[b]	26.43 ± 0.64[c]	24.51 ± 1.15[d]	1.27 ± 0.01[ef]
PGA/4Z4R	17.67 ± 0.06[ef]	18.67 ± 0.76[g]	23.42 ± 0.04[de]	1.48 ± 0.05[def]
PGA/2Z6R	18.24 ± 0.04[ef]	20.96 ± 0.45[ef]	18.45 ± 0.06[fg]	2.35 ± 0.26[b]
PGA/6R2Z	14.02 ± 0.07[f]	16.25 ± 1.25[hi]	21.93 ± 0.25[de]	2.61 ± 0.13[b]
PGA/4R4Z	16.22 ± 0.28[ef]	18.22 ± 0.28[gh]	29.46 ± 0.23[c]	2.53 ± 0.26[b]
PGA/2R6Z	20.07 ± 0.30[cde]	12.48 ± 0.05[k]	17.62 ± 0.05[g]	2.47 ± 0.16[b]
Rha	24.08 ± 1.41[bcd]	30.80 ± 2.05[b]	23.58 ± 0.15[de]	1.23 ± 0.01[ef]
Rha/ZCPs	76.13 ± 7.06[a]	86.46 ± 1.30[a]	120.54 ± 3.69[a]	2.60 ± 0.31[b]
Rha/PGA	15.02 ± 0.93[ef]	16.36 ± 0.53[hi]	13.94 ± 0.17[h]	1.54 ± 0.01[de]
Rha/6Z2P	20.69 ± 1.04[cde]	23.02 ± 1.31[de]	34.49 ± 2.99[b]	3.36 ± 0.34[a]
Rha/4Z4P	25.69 ± 3.62[bc]	23.69 ± 1.69[d]	31.05 ± 3.12[c]	1.16 ± 0.01[ef]
Rha/2Z6P	27.22 ± 5.95[b]	15.15 ± 0.89[ij]	19.67 ± 0.05[fg]	1.75 ± 0.05[cd]
Rha/6P2Z	17.42 ± 1.28[ef]	15.53 ± 0.77[i]	18.84 ± 0.33[fg]	1.12 ± 0.01[f]
Rha/4P4Z	20.78 ± 2.91[cde]	23.16 ± 1.36[de]	29.67 ± 1.71[c]	1.37 ± 0.05[ef]
Rha/2P6Z	17.19 ± 0.33[ef]	20.19 ± 1.18[fg]	122.68 ± 1.52[a]	3.17 ± 0.37[a]

Values are means ± SD (*n* = 3). Different superscript letters in the same column indicate significant differences (*p* < 0.05).

Fig. 3C shows the size distribution of the complex interface-stabilized emulsions using PGA as an inner phase. A serious droplet aggregation occurred in the PGA-stabilized emulsion during thermal treatment with a discrete size distribution. With the incorporation of ZCPs and Rha, the thermal

stability of the emulsions stabilized by the complex interfaces was greatly enhanced with the unimodal size distribution. As depicted in Fig. 3D, Rha/ZCPs showed the most serious droplet aggregation among all the emulsions using Rha as an inner layer due to the strong hydrophobic attraction between the particles. Besides, a slight aggregation between the droplets occurred in the Rha-stabilized emulsion. With the addition of ZCPs and PGA, the thermal stability of the emulsions stabilized by the complex interfaces was enhanced with the monomodal size distribution.

Fig. 3E shows the zeta-potential of the emulsions stabilized by the complex interfaces during thermal treatment, which showed a slight increase in different samples. The coalescence of droplets decreased the specific surface area, which might elevate the concentration of emulsifier adsorbed on an individual droplet with an increased zeta-potential. To achieve a comprehensive insight into the protection of emulsions for nutrients, the retention rate of β-carotene was determined during thermal treatment (Fig. 3F). The β-carotene in the PGA-stabilized emulsion was liable to thermal degradation and the retention rate was 78.65 ± 1.30%. The β-carotene degradation was retarded through controlling the interfacial composition and the mixed PGA-Rha binary emulsifiers greatly improved the thermal stability of β-carotene. Nevertheless, unlike the physical stability of the emulsions stabilized by the complex interface, the combination of particles, biopolymer, and surfactant did not show an obvious improvement on protecting β-carotene from thermal degradation. The droplet aggregation reduced the surface area exposed to chemical reaction of β-carotene degradation, thus restricting the diffusion of pro-oxidants or free radicals into the droplet surface.[31] The β-carotene entrapped in the Rha-stabilized emulsion was also prone to thermal degradation and its retention rate was 79.73 ± 1.99%. When Rha was used as an inner layer, the presence of ZCPs could scarcely protect the entrapped β-carotene effectively, but there was a significant increase in the retention rate of β-carotene in Rha/PGA (87.67 ± 0.49%). Through forming a complex interface by the layer-by-layer technique, Rha, ZCPs, and Rha exerted a synergistic effect on improving the chemical stability of β-carotene in the emulsions. Rha/6P2Z showed the highest retention rate (96.00 ± 0.89%), which was increased by around 21.52% compared to the emulsions stabilized by PGA or Rha alone. These results showed that ZCPs, PGA and Rha provided better protection for the nutrients in the emulsions with Rha as an inner phase compared to PGA as an inner phase.

3.3.4. pH stability The influence of different pH values (2.0, 6.0, and 9.0) on the droplet size and zeta-potential of the emulsions stabilized by the complex interface was investigated (Fig. 4). There existed a slight aggregation in the emulsions at pH 2.0 with increasing droplet size. As reported previously, the dissociation constant (pKa) of PGA is around pH 3.5 and Rha is an anionic biosurfactant with carboxylic groups having pKa around 2.0–3.0.[5,33] In an acidic environment, the zeta-potential decreased close to zero, reducing the electrostatic repulsion between the droplets. When the pH was elevated to 6.0 and 9.0, the complex interface-stabilized emulsions remained very stable with a constant droplet size. The zeta-potential value over |30| mV was acquired with the complex interface and progressive flocculation between the droplets was prevented at pH 6.0.[34] In the presence of particles, biopolymer, and surfactant, the complex interface provided sufficient electrostatic and steric repulsion against droplet aggregation and coalescence, even when the pH was close to pH of zein. Besides, Rha exhibited greater emulsifying ability at pH above 6, which was more efficient to stabilize the interface.[35]
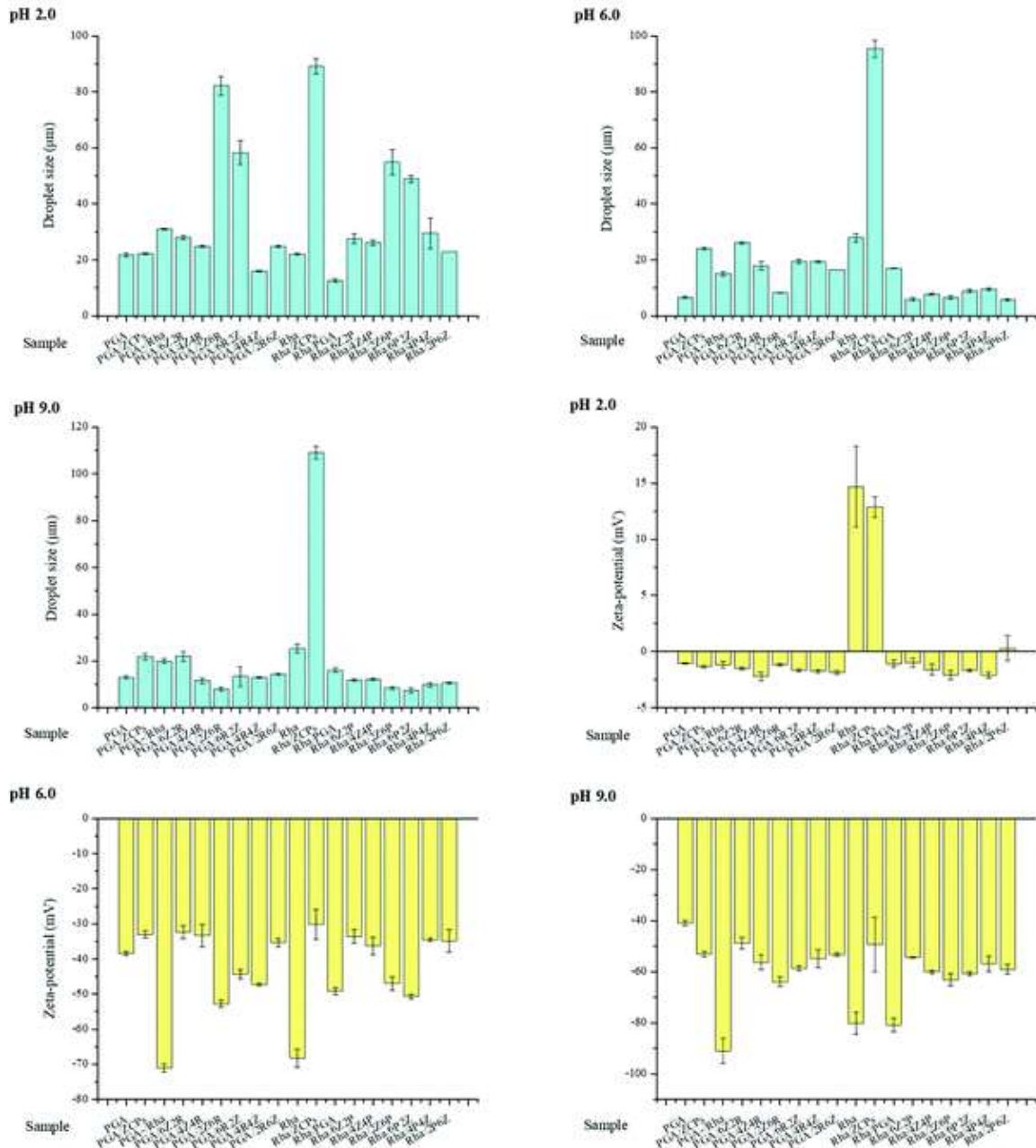
Fig. 4 Effect of pH value on the droplet size and zeta-potential of the emulsions.

3.3.5. Ionic strength stability As depicted in Fig. 5, the stability of the emulsions was investigated under different ionic strengths (10–100 mM). The droplet size of most of the emulsions remained constant at 10 mM except those of PGA/6Z2R, PGA/2R6Z, Rha/ZCPs, and Rha/6Z2P compared to the droplet sizes of the original emulsions (Fig. 1). This phenomenon unraveled that when the interfacial layer contained a higher proportion of ZCPs, the emulsion became more sensitive to salts. This result might be ascribed to the strong hydrophobicity of ZCPs, and the presence of salts reduced the electrostatic repulsion between droplets, thereby promoting the formation of bridges between the particles at the interface, which was consistent with the report of our previous study.[18] With the increase in ionic strength, the droplet size of most of the emulsions was increased slightly. It was noted that the zeta-potential of all the emulsions still remained over |15| mV at 100 mM, which provided sufficient electrostatic repulsion against droplet aggregation. As aforementioned, there was an

obvious increase in the emulsions with a higher level of ZCPs as an outer layer. When ZCPs were in the outer layer of the interface or the proportion was high, the emulsion with the complex interface was unstable under a high ionic strength. Therefore, the addition sequence and mass ratio of different stabilizers required to be precisely regulated therefore the complex interface could cope with the needs of emulsions in different environments.
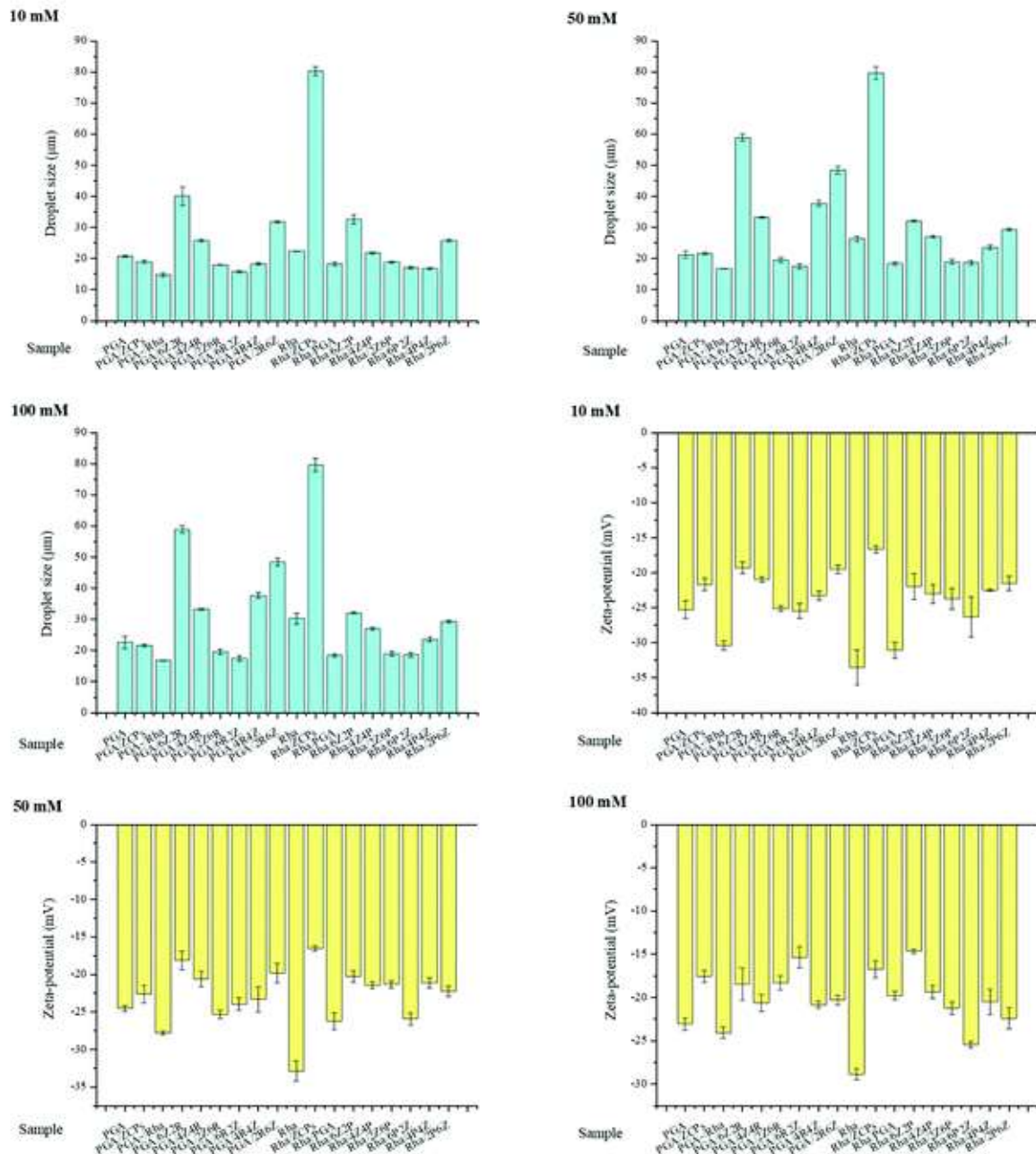
Fig. 5 Effect of ionic strength on the droplet size and zeta-potential of the emulsions.

3.4. Morphological observation

3.4.1. CLSM Through the observation of CLSM, the PGA-stabilized emulsion exhibited small spherical droplets without any aggregation (Fig. 6). With the addition of ZCPs, there was a slight aggregation between droplets with an increase in size due to hydrophobic attraction. Nevertheless, the droplet

size of PGA/Rha was much smaller and uniform. At a higher ZCPs level, the droplet size of PGA/6Z2P was increased but the droplets were separated by the steric hindrance of particles. By decreasing the ZCP level and increasing the Rha level, the droplet size was slightly reduced but the emulsions tended to aggregate owing to the weakening of spatial repulsion. When Rha was added firstly to the PGA-stabilized interface and then ZCPs, the droplet size was further decreased. Additionally, it was observed that the increasing level of ZCPs gradually separated the droplets and excess particles entered into the aqueous phase and formed some larger aggregates.
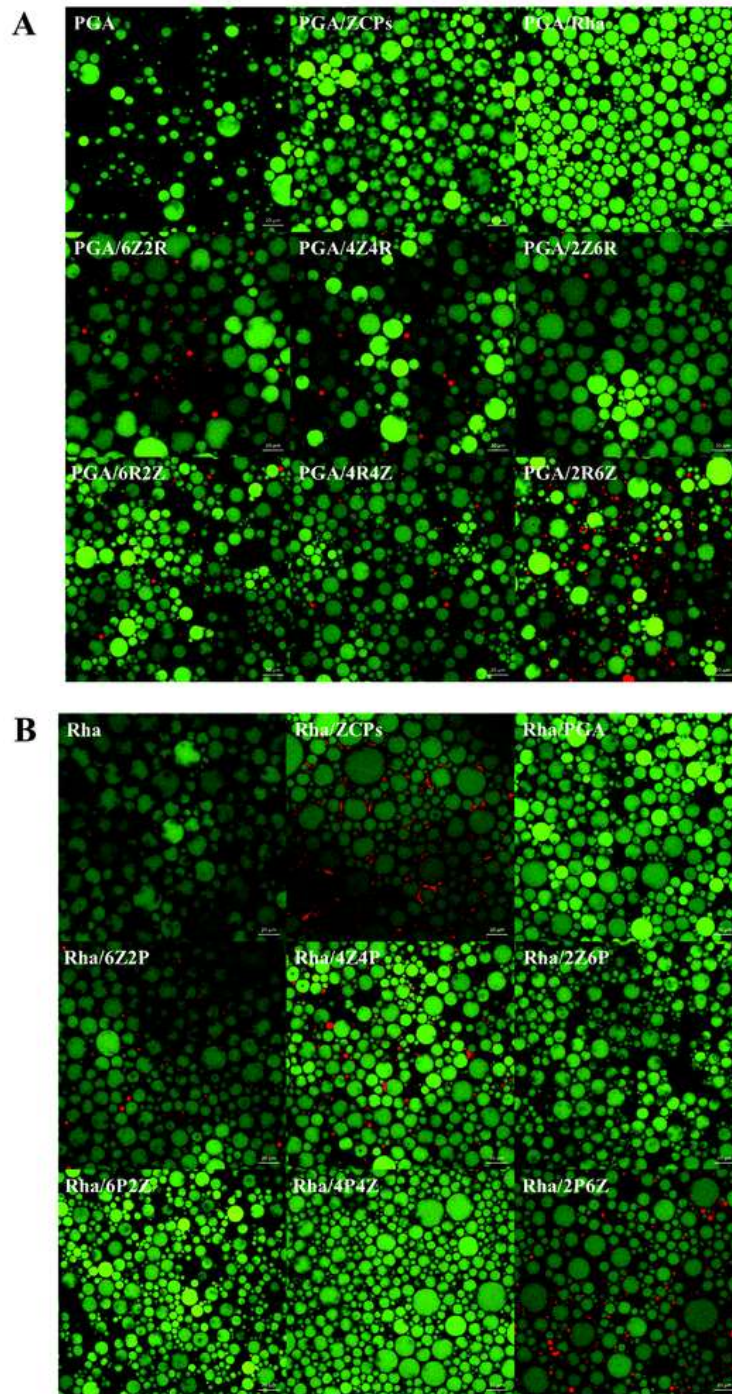
Fig. 6 CLSM image of the complex interface-stabilized emulsions using PGA (A) or Rha (B) as an inner layer.

Compared to the PGA-stabilized emulsion, the Rha-stabilized emulsion was slightly aggregated with a larger droplet size. With the incorporation of ZCPs, it was observed that the particles fully filled the inter-droplet gaps as an outer layer of interface, acting as bridges between the droplets. The combination of Rha and PGA showed a synergistic effect on the stabilization of the emulsions with a decreased droplet size. When ZCPs were added firstly to the Rha-stabilized interface and then PGA, the particles formed bridges between the droplets eventually constituting a network structure. Nevertheless, with the decrease in the ZCP level and the rise in the PGA level, the particles between droplets were reduced but the emulsion still maintained a network structure.[16] A similar phenomenon was observed in the complex interface-stabilized emulsions with ZCPs as an outer layer. At a low level of ZCPs, the smaller droplets were aggregated in the emulsions. With increasing the ZCP level, the obvious particle bridges occurred between the droplets with a constant size, revealing that the close-packing of particles provided sufficient steric hindrance to stabilize the droplets through the arrested coalescence mechanism.[36] The network structure formed at the interfaces of the emulsions by particle bridging further enhanced the emulsion stability.[18,28]

3.4.2. Cryo-SEM Cryo-SEM can be used to acquire the three-dimensional structure of different emulsions.[5] As demonstrated in Fig. 7A, the PGA-stabilized emulsion droplets showed a smooth surface. With the addition of ZCPs, a number of particles occupied the droplet surface to provide steric repulsion. Nevertheless, excess ZCPs could enter into the aqueous phase and induce bridging flocculation between the droplets. The combination of PGA and Rha stabilized the emulsion droplets with the appearance of a smooth surface. As PGA, ZCPs, and Rha were co-adsorbed on the interface, the complex interface exhibited some particular interfacial structures. When ZCPs were added firstly and then Rha, a clear fibrous structure was formed between the particles. This fibrous structure might be formed by the electrostatic and hydrophobic interactions between Rha and particles, especially at a higher mass ratio of ZCPs to Rha. The interfacial film consisted of a network structure composed of the particles and surfactant tightly wrapping the emulsion droplets. With decreasing the mass ratio of ZCPs to Rha, the fibrous structure at the interface gradually disappeared. When Rha was added firstly to the PGA-stabilized interface and then ZCPs, it was found that some particles scattered on the droplet surface without obvious aggregation at lower mass ratios of ZCPs to Rha. With the increase in ZCP content, a honeycomb-like structure appeared on the droplet surface, which was different from the fibrous structure when ZCPs was added firstly and then Rha. This phenomenon indicated that when Rha was added firstly, and it was preferentially co-adsorbed to the surface of droplets with PGA instead of reacting with particles or forming bridges between the particles. The ZCPs in the outer layer of the interface tended to aggregate due to the attractive force between the particles and formed a different interfacial structure.

The Rha-stabilized emulsion demonstrated spherical droplets with a smooth surface, which was similar to the PGA-stabilized emulsion (Fig. 7B). With the incorporation of ZCPs, the honeycomb-like structure appeared at the interface formed by the aggregation of colloidal particles. The addition of PGA onto the Rha-stabilized droplets had scarcely a significant influence on the interfacial structure with a smooth surface. Nevertheless, the mass ratio of ZCPs and PGA possessed a great impact on the interfacial structure of emulsion droplets with Rha as an inner layer. When ZCPs were added firstly and then PGA, a denser network structure was formed at the interface, indicating that the outer PGA molecules connected adjacent particles through electrostatic and hydrophobic attractions.[18] With increasing the PGA content and decreasing the particle level, there were fewer bridges between the particles and the network structure at the interface gradually disappeared and transformed into a gully-like morphology. At the same mass ratio of ZCPs and PGA, Rha/6P2Z exhibited a rougher surface of the droplets than Rha/2Z6P through changing the adding sequence. This phenomenon showed that when PGA was used as the outer layer, the particle layer at the interface was well covered. When ZCPs

were on the outer layer at the interface, the particles or aggregates attached to the droplet surface were clearly observed through cryo-SEM. The morphology of the droplet surface was consistent with the mass ratio and adding sequence of the surfactant, biopolymer and particles in the fabrication of the emulsions stabilized by the complex interface.
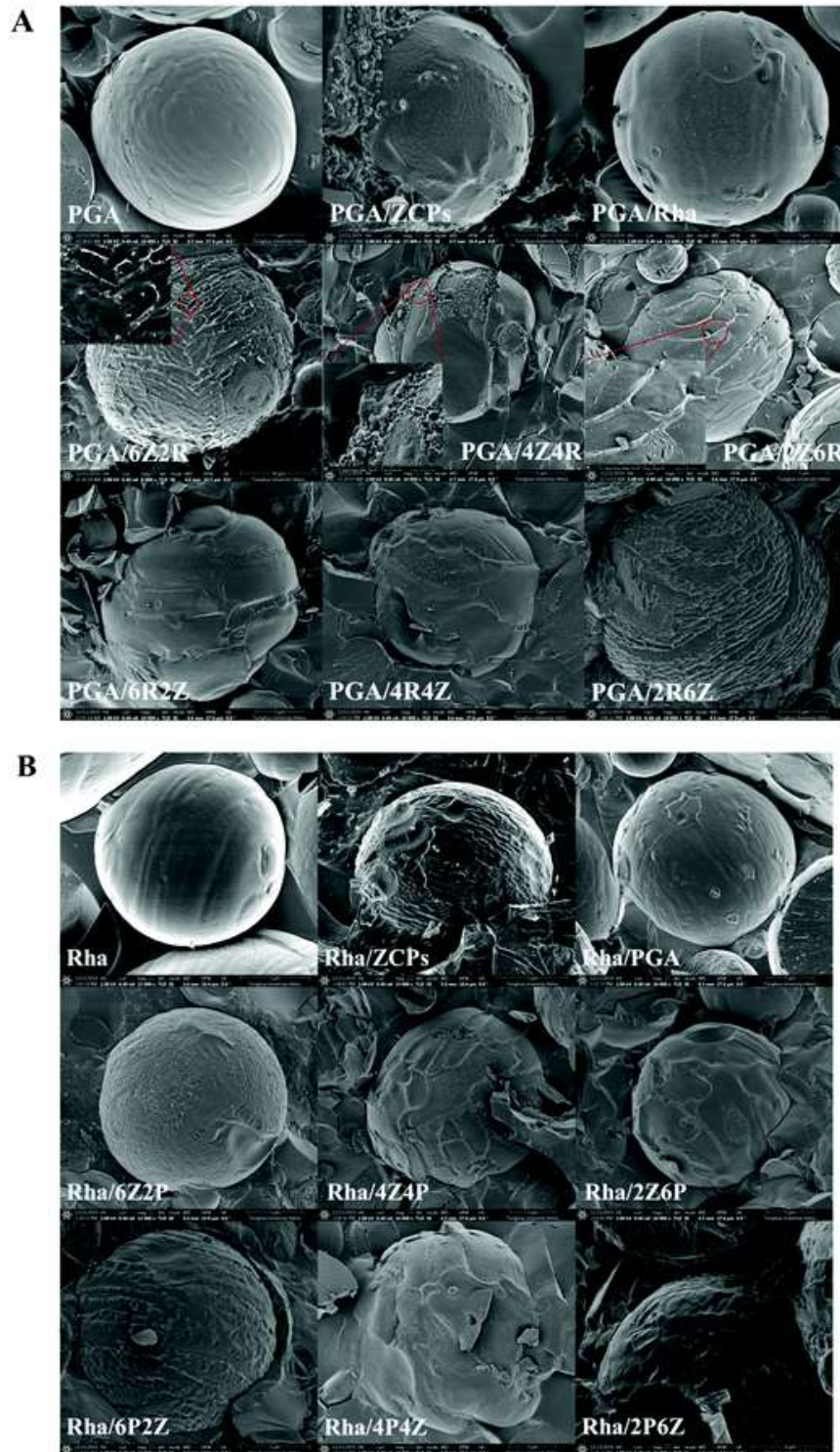
Fig. 7 Cryo-SEM microstructure of the complex interface-stabilized emulsions using PGA (A) or Rha (B) as an inner layer.

3.5. Rheological properties

3.5.1. Apparent viscosity Although many researchers studied the rheology of the emulsions stabilized by individual surfactants, biopolymers or particles, the rheological properties of the emulsions with the mixed biopolymer–surfactant–particle interface have never been reported before. The PGA-stabilized emulsion showed a low viscosity due to its smaller droplet size and strong repulsion between the droplets (Fig. 8A). With the incorporation of Rha or ZCPs, there was a slight decrease in the emulsion viscosity, since the competitive adsorption between PGA and Rha or ZCPs reduced the stability of the interfacial membrane, disrupting the interaction between PGA molecules. When ZCPs were added firstly to the PGA-stabilized interface, the emulsion viscosity was increased slightly. Nevertheless, when Rha was added firstly and then ZCPs, the emulsion viscosity was decreased especially at higher levels of Rha. Through the observation by cryo-SEM (Fig. 7), when Rha was on the outer layer, the particles and surfactant formed a fibrous structure at the interface through electrostatic and hydrophobic attractions. The network structure composed of the particles and surfactant wrapped the droplets and increased the viscosity. When Rha was added firstly to the PGA-stabilized interface, it could co-adsorb onto the droplet surface with PGA competitively through organic displacement,[2] which caused the instability of the interfacial film and a decrease in the emulsion viscosity.
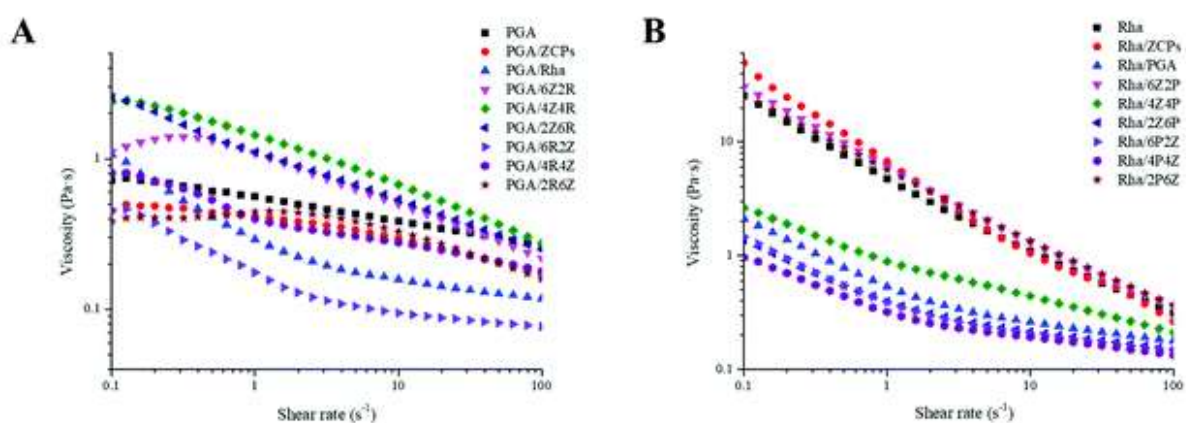
Fig. 8 Apparent viscosity of the emulsions using PGA (A) or Rha (B) as an inner layer.

The Rha-stabilized emulsion showed a higher viscosity than the PGA-stabilized one (Fig. 8B). As aforementioned, the larger droplet size and the weaker repulsive force between the droplets facilitated droplet aggregation and enhanced the viscosity.[37] The adsorption of ZCPs to the Rha-stabilized interface increased the emulsion viscosity slightly due to the hydrophobic attraction between the droplets with particles.[32] Nonetheless, the addition of PGA into the Rha-stabilized interface decreased the emulsion viscosity, revealing that the presence of PGA improved the stability of the interfacial membrane and prevented droplet aggregation. In terms of the emulsions co-stabilized by the surfactant, particle and polymer, the addition order and mass ratio of ZCPs and PGA exerted an important impact on the viscosity. When ZCPs were added firstly to the Rha-stabilized interface and then PGA, the emulsion viscosity was gradually decreased with the increase in the PGA content. Similarly, when PGA was added firstly to the Rha-stabilized interface and then ZCPs, there was an obvious increase in the emulsion viscosity with the rise in the ZCP level. These results interpreted that when PGA was located in the outer layer of the emulsion, the repulsive force between the droplets was increased and the droplet size became smaller, which reduced the emulsion viscosity.

While the particles were in the outer layer, the attractive force between the droplets was enhanced and the droplets tended to aggregate, thus increasing the emulsion viscosity.[16]
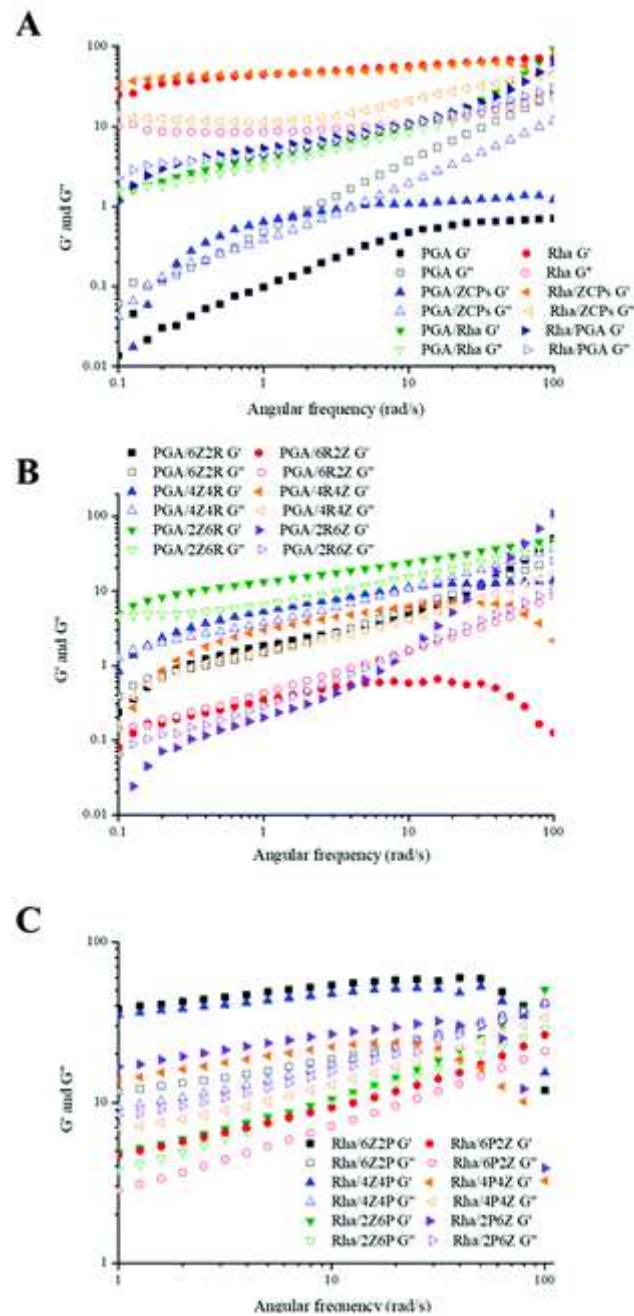
Fig. 9 Viscoelasticity of the emulsions stabilized by PGA, PGA/ZCPs, PGA/Rha, Rha, Rha/ZCPs and Rha/PGA (A); viscoelasticity of the emulsions using PGA (B) or Rha (C) as an inner layer.

3.5.2. Viscoelastic properties As depicted in Fig. 9A, the *G'* was much lower than *G''* in the PGA-stabilized emulsion, indicating a characteristic liquid-like behaviour. With the incorporation of ZCPs into the PGA-covered interface, the *G'* of PGA/ZCPs was increased and entangled with *G''*. This result revealed a transition of the emulsions from liquid-like to solid-like behaviour, interpreting that the droplets easily formed bridges and aggregated with ZCPs as an outer layer.[5] Interestingly, the *G'* of PGA/Rha was further increased and showed a similar value to *G''*. This phenomenon might be

explained by that the presence of Rha caused the competitive adsorption between Rha and PGA at the interface, thereby resulting in the emulsion aggregation.[2] In terms of the Rha-stabilized emulsion, the G' was much higher than G'', indicating a characteristic solid-like behaviour due to the serious aggregation of droplets. With the adsorption of particles, Rha/ZCPs still maintained high elasticity. Nevertheless, when PGA was adsorbed on the outer layer of the Rha-stabilized interface, the G' of PGA/ZCPs was greatly decreased and entangled with G'', indicating a transition of the emulsions from solid-like to liquid-like behaviour. The addition of PGA provided sufficient electrostatic and steric repulsion to prevent droplet aggregation and the decrease of the droplet size. It was noted that the viscoelasticity of Rha/PGA was different from that of PGA/Rha, showing the importance of the adding sequence of different types of emulsifiers.

In the presence of the biopolymer, particles, and surfactant, both G' and G'' of PGA/6Z2R were increased when Rha was added as an outer layer compared to PGA/ZCPs (Fig. 9B). With the rise of the Rha concentration, both G' and G'' of the emulsions were elevated continuously and the G' was slightly larger than G'', which was similar to PGA/Rha. The Rha as an outer layer increased the hydrophobic attraction and promoted the bridging flocculation between the droplets. When ZCPs were on the outer layer, the adsorption of particles onto the interface gradually increased the elasticity of the emulsions. At lower levels of ZCPs, it was observed that the G' decreased at higher shear rates, testifying that the aggregation of the emulsion was reversible and easily destroyed. At higher levels of ZCPs, the G' increased with the rise of the shear rate and was greater than G'', indicating that the emulsion droplets were bridged and aggregated due to the hydrophobic attraction between the particles with a solid-like behavior.[5,18]

Fig. 9C shows the viscoelasticity of the complex interface-stabilized emulsions with Rha as an inner layer. When ZCPs were firstly added to the Rha-stabilized interface and then PGA, the G' was much higher than G'' in the emulsion, indicating a characteristic solid-like behaviour especially at a higher level of ZCPs. With the decrease in the mass ratio of ZCPs to PGA, the G' of the emulsion was gradually decreased and entangled with G'', indicating a transition of the emulsions from solid-like to liquid-like behaviour. A similar phenomenon occurred in the complex interface-stabilized emulsions when PGA was added firstly to the Rha-stabilized interface and then ZCPs. With the increase of the ZCP level, the G' of the complex interface-stabilized emulsion increased and was greater than the G''. The presence of particles in the complex interface increased the interfacial thickness, improved the elasticity of the interface, and strengthened the attraction between the droplets, forming the network structure in the emulsion with gel-like properties.[38] Conversely, the biopolymer (PGA) strengthened the repulsion between the droplets, thereby reducing the bridging between the droplets.[16,28]

3.6. *In vitro* gastrointestinal digestion of β-carotene loaded emulsions

3.6.1. Droplet size The droplet size of the PGA-stabilized emulsion remained stable during gastric digestion, which was similar to that of PGA/Rha (Table 1). Nevertheless, there was a serious aggregation of PGA/ZCPs in the gastric phase, and the droplet size increased from 20.23 ± 0.27 to 120.54 ± 3.69 μm, which was attributed to two aspects: firstly, when the emulsion was mixed with SGF, pepsin catalyzed the proteolysis of ZCPs in the outer layer of the interface into peptide fragments, thus weakening the steric hindrance and promoting the aggregation between the droplets. Secondly, in the acidic environment, the electrostatic complexation between PGA and ZCPs diminished, which reduced the stability of the interfacial layer.

In terms of the emulsions co-stabilized by PGA, ZCPs, and Rha with PGA as an inner layer, the droplet size remained stable in the gastric phase when ZCPs were added firstly and then Rha (Table 1). Interestingly, when ZCPs were on the outer layer, the droplet size of the emulsions was greatly increased. This phenomenon unraveled that the hydrolysis of zein disintegrated the particle layer in

the presence of pepsin and promoted the droplet coalescence. When Rha was used as an outer layer, the emulsions with the complex interface exhibited a better gastric stability due to the coating of Rha limiting the access of pepsin to the binding sites of zein, which protected ZCPs from proteolysis.[16]

After gastric digestion, the droplet size of the Rha-stabilized emulsion remained stable, which was similar to that of Rha/PGA. A significant increase was observed in the droplet size of Rha/ZCPs from 76.13 ± 7.06 to 120.54 ± 3.69 μm. In terms of the emulsion stabilized by the complex interface with Rha as an inner layer, as the mass ratio of ZCPs to PGA was increased, the increase in the droplet size was larger and the emulsion became more unstable in the gastric phase, regardless of the order of ZCPs and PGA. As aforementioned, the pepsin in SGF facilitated the proteolysis of ZCPs, which reduced the steric hindrance and promoted the coalescence between the droplets. When PGA was located in the outer layer, the emulsions with the complex interface exhibited a better gastric stability with the increase in the PGA level. The protection of PGA decreased the hydrolysis of the protein particle layer and provided sufficient repulsion to prevent the emulsion coalescence. After the digesta entered into the small intestinal phase, an obvious decrease of the droplet size occurred in all the emulsions. The presence of pancreatin, bile salts, and lipase might destroy the aggregation between the droplets and facilitate the emulsification of droplets. The particle layer of the interface was further hydrolyzed and disrupted by pancreatin and bile salts.[39] In a neutral pH environment, Rha exhibited a higher emulsifying activity to promote further a reduction of the droplet size.[35] Furthermore, lipolytic products could accumulate on the interface and affect the droplet bridging.[16,39]

The droplet size distribution of all the emulsions during different digestion times is presented in Fig. 10 and 11. In terms of the emulsions with PGA as an inner layer, there was an obvious aggregation in PGA/ZCPs, PGA/6Z2R, PGA/4Z4R, and PGA/2R6Z, which were mainly the emulsions with ZCPs on the outer layer or with a higher proportion of ZCPs (Fig. 10). The phenomenon showed that the presence of ZCPs in the interfacial layer could easily induce droplet aggregation in the gastric phase. When Rha was on the inner layer of the emulsions, a serious droplet aggregation was observed in Rha/ZCPs, Rha/6Z2P, Rha/4P4Z, and Rha/2P6Z (Fig. 11). The hydrolysis of protein particles promoted the aggregation of droplets, but the coating of the PGA layer could enhance the emulsion stability and inhibit the proteolysis of ZCPs.[40]
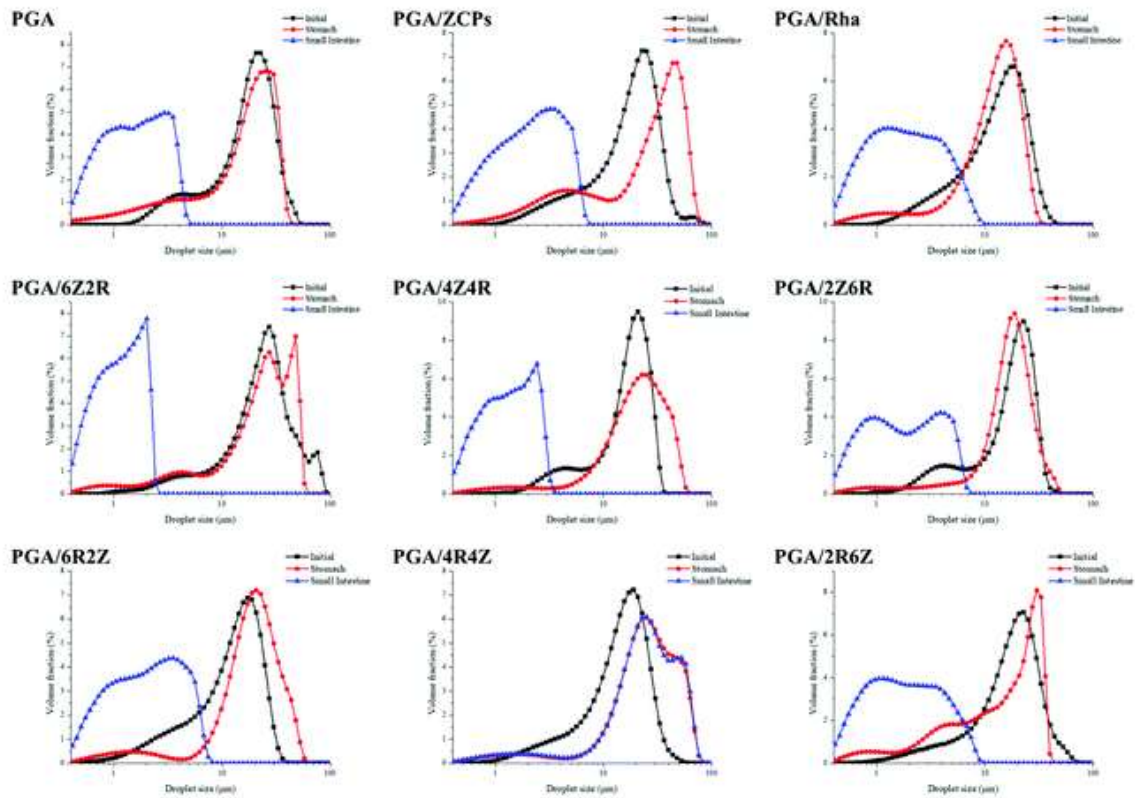
Fig. 10 Digestion time dependence of droplet size distribution of the emulsions using PGA as an inner layer.
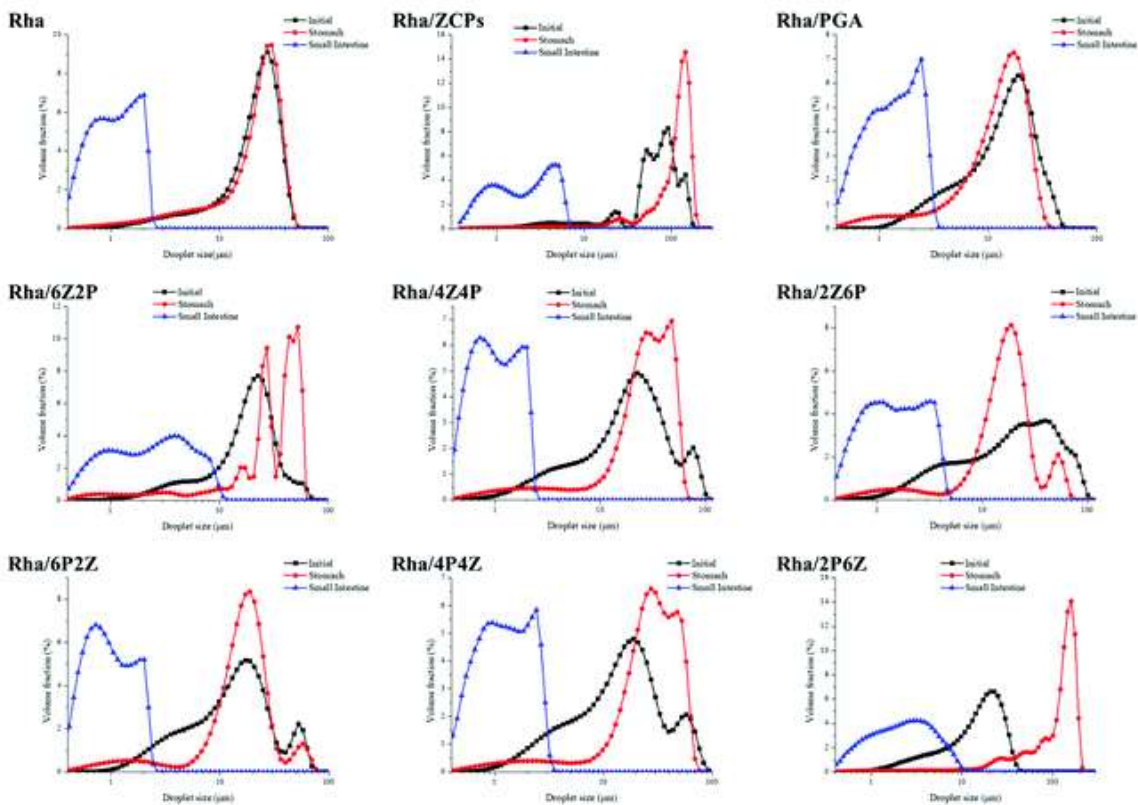
Fig. 11 Digestion time dependence of droplet size distribution of the emulsions using Rha as an inner layer.

3.6.2. Lipid digestion The impact of interfacial compositions on the lipolysis was evaluated by determining the release rate of FFAs generated within the small intestinal phase over time. The PGA-stabilized emulsion exhibited a relatively high FFA release (23.41%) after intestinal digestion (Fig. 12A). With the incorporation of ZCPs, the FFA release rate of PGA/ZCPs was slightly decreased to 22.34%. When Rha was added to the PGA-stabilized interface, the FFA release rate of PGA/Rha was increased to the maximum (24.26%) among all the emulsions. These results were consistent with the physicochemical stability and interfacial structure of the emulsions, revealing that the existence of particles at the interface restricted the adsorption of bile salts and lipase to the droplet surface through steric repulsion. Meanwhile, the competitive displacement between the biopolymer and surfactant was detrimental to the stability of the interfacial layer of the emulsions, which further facilitated the lipolysis.[13,26] Compared to PGA/ZCPs and PGA/Rha. The co-existence of PGA, ZCPs, and Rha showed a synergistic effect on delaying the lipolysis of the complex interface-stabilized emulsions. When ZCPs was added firstly to the PGA-covered interface, the FFA release rates of PGA/6Z2R, PGA/4Z4R, and PGA/2Z6R were reduced to 16.84%, 20.38%, and 18.64%, respectively. This phenomenon indicated that there were substantial interfacial gaps between the adsorbed particles and the addition of Rha could enter into the interfacial gaps, thus inhibiting the adsorption of bile salts and lipase to the droplet surface through the interfacial gaps.[15,16] When Rha was added firstly and then ZCPs, the FFA release rates of PGA/6R2Z, PGA/4R4Z, and PGA/2R6Z were 24.95%, 21.25%, and 23.83%, respectively, which were relatively higher than those of the emulsions with Rha as an outer layer. On one hand, the bile salts and lipase could penetrate the interfacial film through the gaps between the particles. On the other hand, the competitive adsorption of PGA and Rha caused the instability of the interface, which facilitated the adsorption of bile salts and lipase onto the droplet surface.[40,41]

Compared to the PGA-stabilized emulsion, the Rha-stabilized emulsion showed a much lower FFA release rate (17.05%), which might be attributed to that its aggregated state hindered the access of bile salts and lipases (Fig. 12B). With the adsorption of ZCPs and PGA, the FFA release rates of Rha/ZCPs and Rha/PGA were shifted to 17.91% and 16.51%, indicating that the PGA layer was more resistant to the competitive adsorption and hydrolysis of bile salts and lipases than the ZCPs layer. The particle layer (ZCPs) could be hydrolyzed in the gastric and intestinal phases by pepsin and pancreatin. Comparably, the PGA layer carried a substantial negative charge at pH 6.8, which provided the strong electrostatic repulsion between PGA and bile salts and restricted the access of bile salts onto the droplet surface.[16] A similar phenomenon was found in the emulsions using the mixed surfactant–particle–biopolymer interface. When PGA was on the outer layer of the emulsions, the FFA release rate was decreased from 17.24% (Rha/6Z2P) to 14.95% (Rha/2Z6P) with the increase in the PGA level. Similarly, when PGA was added firstly to the Rha-stabilized interface and then ZCPs, there was a continuous increase in the FFA release rate from 12.59% (Rha/6P2Z) to 17.91% (Rha/2P6Z) with the rise of the ZCP proportion. The adsorption of PGA at the interface was more efficient to delay the fat digestion in the small intestine than that of ZCPs. On one hand, ZCPs could be hydrolyzed in the gastrointestinal tract by proteases, which failed to provide consistent steric repulsion. On the other hand, the coating of PGA produced strong electrostatic repulsion to retard the adsorption and displacement of negatively charged bile salts and lipases in the neutral environment.[13]
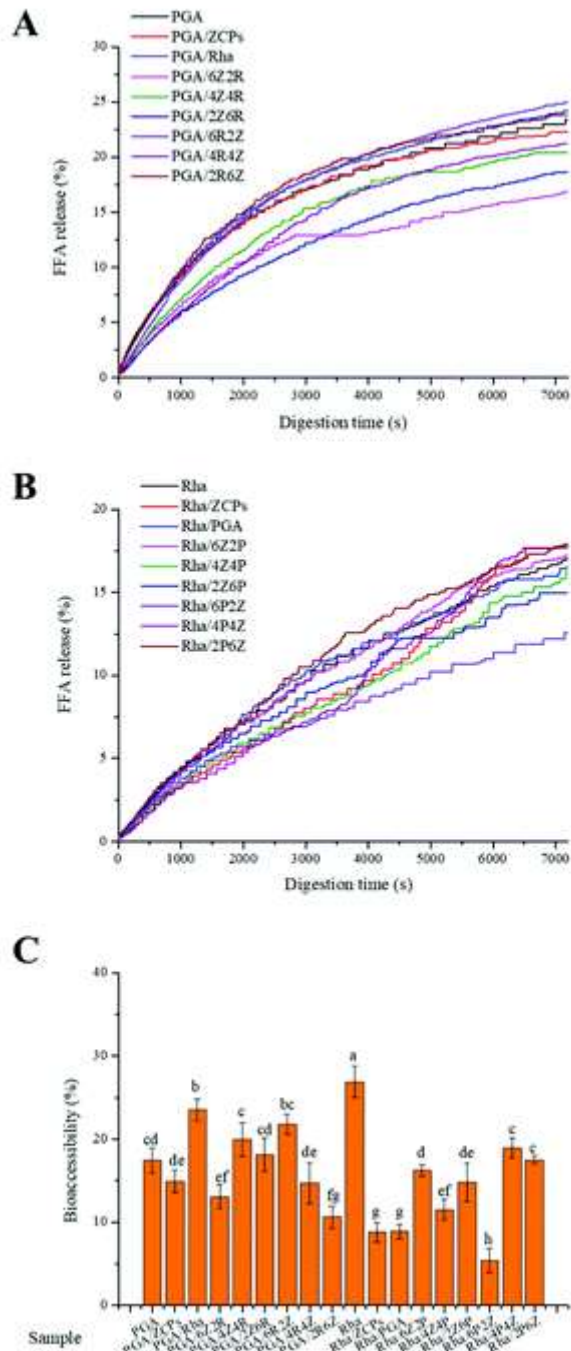
Fig. 12 Digestion time dependence of FFA release (%) from the emulsions using PGA (A) or Rha (B) as an inner layer; bioaccessibility of β-carotene entrapped in the emulsions (C).

3.6.3. Bioaccessibility of β-carotene The release and solubilization of lipophilic nutrients occur for the most part in the small intestine and are affected by several exogenous factors, such as properties of nutrients, food processing, interfacial composition, and so forth.[42] The solubilization capacity of the mixed micelles formed is the determining factor of bioaccessibility by calculating the concentration of nutraceuticals in the micellar phase.[42,43] The bioaccessibilities of β-carotene in Rha, Rha/ZCPs, and Rha/PGA were 17.43 ± 1.49%, 14.92 ± 1.31% and 23.51 ± 1.32%, respectively, which was consistent with the FFA release of the emulsions (Fig. 12C). In terms of the emulsions co-stabilized by PGA, ZCPs, and Rha, when ZCPs were added firstly to the PGA-stabilized interface, the β-carotene

bioaccessibilities in PGA/6Z2R, PGA/4Z4R, and PGA/2Z6R were 13.10 ± 1.45%, 19.98 ± 2.02%, and 18.12 ± 2.00%, respectively. The mixed micelles in the small intestine were composed of the FFAs, bile salts and other surface-active substances, therefore the level of FFAs released was the most important endogenous factor to determine the solubilization capacity of the mixed micelles.[39,44] The incorporation of Rha facilitated the formation and stabilization of the mixed micelles, which showed a better impact on improving the bioaccessibility of β-carotene than PGA or ZCPs.[16] With the increase in the ZCP level, the β-carotene bioaccessibility decreased from 21.82 ± 1.18% (PGA/6R2Z) to 10.63 ± 1.33% (PGA/2R6Z) when ZCPs were on the outer layer.

Compared to the PGA-stabilized emulsion, the Rha-stabilized emulsion showed a higher β-carotene bioaccessibility (26.89 ± 1.86%), despite the former having a higher FFA release rate (Fig. 12C). The result suggested that the incorporation of Rha at the interface indeed promoted the formation of the mixed micelles and improved the nutrient bioaccessibility. Nevertheless, the addition of ZCPs and PGA reduced the β-carotene bioaccessibility in Rha/ZCPs and Rha/PGA to 8.78 ± 1.12% and 8.88 ± 0.89%. Unlike Rha, both ZCPs and PGA restricted the dissolution of β-carotene into the mixed micelles formed after the digestion of the emulsions in the small intestine. The hydrophobic residues of ZCPs could complex with β-carotene through hydrophobic attraction.[42] Additionally, PGA and bile salts could generate strong electrostatic repulsion, and therefore both ZCPs and PGA could restrict the formation of the mixed micelles or the dissolution of β-carotene.[39,45] When ZCPs were added firstly to the Rha-stabilized interface and then PGA, there was a slight decline of β-carotene bioaccessibility from 16.24 ± 0.66% (Rha/6Z2P) to 14.80 ± 2.29% (Rha/2Z6P). When the complex interface-stabilized emulsions had ZCPs as an outer layer, the β-carotene bioaccessibility was elevated from 5.41 ± 1.51% (Rha/6P2Z) to 17.49 ± 0.52% (Rha/2P6Z), which was consistent with the release of FFA (Fig. 12B). The phenomenon suggested that PGA showed a greater effect on β-carotene bioaccessibility in the emulsions than ZCPs. Owing to its large molecular weight and better digestion stability, PGA provided strong steric hindrance and electrostatic repulsion for the droplets to prevent the adsorption of bile salts, which further delayed the lipid digestion and reduced the release of FFA while decreasing the bioaccessibility of β-carotene.[13,44]

4. Conclusion

In summary, we proposed a novel stabilization mechanism of the emulsions containing biopolymers, surfactants, and particles. The stability, microstructure, and *in vitro* gastrointestinal digestion of the complex interface-stabilized emulsions were investigated. When the emulsifiers (PGA and Rha) were combined with particles (ZCPs) as surface active agents, there existed a synergistic effect on enhancing the stability of O/W emulsions using the complex interfaces. The application of triple emulsifiers for the development of β-carotene loaded O/W emulsions was firstly demonstrated. These findings underlined the importance of regulating the interactions between the interfacial stabilizers, which was achieved by controlling the addition sequence and mass ratio of multiple stabilizers. In comparison with either Pickering emulsions or conventional ones, the complex interface-stabilized emulsions exhibited enhanced stability and delayed lipolysis. The complex interface-stabilized emulsions show promising potential for applications in foods for controlled lipid digestion or nutrient delivery purposes.

Conflicts of interest
The authors declare no competing financial interest.

Acknowledgements

References

D. J. McClements and C. E. Gumus , Natural emulsifiers—Biosurfactants, phospholipids, biopolymers, and colloidal particles: Molecular and physicochemical basis of functional performance, Adv. Colloid Interface Sci., 2016, 234 , 3 —26.

L. A. Pugnaloni , E. Dickinson , R. Ettelaie , A. R. Mackie and P. J. Wilde , Competitive adsorption of proteins and low-molecular-weight surfactants: computer simulation and microscopic imaging, Adv. Colloid Interface Sci., 2004, 107 , 27 —49

Y. Li and D. Julian McClements , New Mathematical Model for Interpreting pH-Stat Digestion Profiles: Impact of Lipid Droplet Characteristics on in Vitro Digestibility, J. Agric. Food Chem., 2010, 58 , 8085 —8092

X. Chen , D. J. McClements , J. Wang , L. Zou , S. Deng , W. Liu , C. Yan , Y. Zhu , C. Cheng and C. Liu , Coencapsulation of (-)-Epigallocatechin-3-gallate and Quercetin in Particle-Stabilized W/O/W Emulsion Gels: Controlled Release and Bioaccessibility, J. Agric. Food Chem., 2018, 66 , 3691 —3699

Y. Wei , Z. Yu , K. Lin , S. Yang , K. Tai , J. Liu , L. Mao , F. Yuan and Y. Gao , Fabrication, Physicochemical Stability, and Microstructure of Coenzyme Q10 Pickering Emulsions Stabilized by Resveratrol-Loaded Composite Nanoparticles, J. Agric. Food Chem., 2020, 68 , 1405 —1418

D. Liu , N. Xue , L. Wei , Y. Zhang , Z. Qin , X. Li , B. P. Binks and H. Yang , Surfactant Assembly within Pickering Emulsion Droplets for Fabrication of Interior-Structured Mesoporous Carbon Microspheres, Angew. Chem., Int. Ed., 2018, 57 , 10899 —10904

B. P. Binks , A. Desforges and D. G. Duff , Synergistic stabilization of emulsions by a mixture of surface-active nanoparticles and surfactant, Langmuir, 2007, 23 , 1098 —1106

H. Firoozmand , B. S. Murray and E. Dickinson , Interfacial structuring in a phase-separating mixed biopolymer solution containing colloidal particles, Langmuir, 2009, 25 , 1300 —1305

P. Oymaci and S. A. Altinkaya , Improvement of barrier and mechanical properties of whey protein isolate based food packaging films by incorporation of zein nanoparticles as a novel bionanocomposite, Food Hydrocolloids, 2016, 54 , 1 —9

M. Xu , J. Jiang , X. Pei , B. Song , Z. Cui and B. P. Binks , Novel Oil-in-Water Emulsions Stabilised by Ionic Surfactant and Similarly Charged Nanoparticles at Very Low Concentrations, Angew. Chem., Int. Ed., 2018, 57 , 7738 —7742

P. G. Arkoumanis , I. T. Norton and F. Spyropoulos , Pickering particle and emulsifier co-stabilised emulsions produced via rotating membrane emulsification, Colloids Surf., A, 2019, 568 , 481 —492

L. Pinďáková , V. Kašpárková and R. Bordes , Role of protein-cellulose nanocrystal interactions in the stabilization of emulsion, J. Colloid Interface Sci., 2019, 557 , 196 —206

A. Sarkar , S. Zhang , M. Holmes and R. Ettelaie , Colloidal aspects of digestion of Pickering emulsions: Experiments and theoretical models of lipid digestion kinetics, Adv. Colloid Interface Sci., 2019, 263 , 195 —211

A. Sarkar , H. Li , D. Cray and S. Boxall , Composite whey protein–cellulose nanocrystals at oil-water interface: Towards delaying lipid digestion, Food Hydrocolloids, 2018, 77 , 436 —444

Y. Wei , Z. Tong , L. Dai , P. Ma , M. Zhang , J. Liu , L. Mao , F. Yuan and Y. Gao , Novel colloidal particles and natural small molecular surfactants co-stabilized Pickering emulsions with hierarchical interfacial structure: Enhanced stability and controllable lipolysis, J. Colloid Interface Sci., 2020, 563 , 291 —307

Y. Wei , Z. Tong , L. Dai , D. Wang , P. Lv , J. Liu , L. Mao and F. Yuan , Influence of interfacial compositions on the microstructure, physiochemical stability, lipid digestion and β -carotene bioaccessibility of Pickering emulsions, Food Hydrocolloids, 2020, 104 , 105738

A. Sarkar , V. Ademuyiwa , S. Stubley , N. H. Esa , F. M. Goycoolea , X. Qin , F. Gonzalez and C. Olvera , Pickering emulsions co-stabilized by composite protein/polysaccharide particle-particle interfaces: Impact on in vitro gastric stability, Food Hydrocolloids, 2018, 84 , 282 —291

Y. Wei , C. Sun , L. Dai , L. Mao , F. Yuan and Y. Gao , Novel Bilayer Emulsions Costabilized by Zein Colloidal Particles and Propylene Glycol Alginate. 2. Influence of Environmental Stresses on Stability and Rheological Properties, J. Agric. Food Chem., 2019, 67 , 1209 —1221

A. R. Patel and K. P. Velikov , Zein as a source of functional colloidal nano- and microstructures, Curr. Opin. Colloid Interface Sci., 2014, 19 , 450 —458

Y. Wei , C. Sun , L. Dai , X. Zhan and Y. Gao , Structure, physicochemical stability and in vitro simulated gastrointestinal digestion properties of β-carotene loaded zein-propylene glycol alginate composite nanoparticles fabricated by emulsification-evaporation method, Food Hydrocolloids, 2018, 81 , 149 —158

Y. Wei , S. Yang , L. Zhang , L. Dai , K. Tai , J. Liu , L. Mao , F. Yuan , Y. Gao and A. Mackie , Fabrication, characterization and in vitro digestion of food grade complex nanoparticles for co-delivery of resveratrol and coenzyme Q10, Food Hydrocolloids, 2020, 105 , 105791

C. P. Tan and M. Nakajima , β-Carotene nanodispersions: Preparation, characterization and stability evaluation, Food Chem., 2005, 92 , 661 —671

P. Sriamornsak , N. Thirawong , K. Cheewatanakornkool , K. Burapapadh and W. Sae-Ngow , Cryo-scanning electron microscopy (cryo-SEM) as a tool for studying the ultrastructure during bead formation by ionotropic gelation of calcium pectinate, Int. J. Pharm., 2008, 352 , 115 —122

M. Minekus , M. Alminger , P. Alvito , S. Ballance , T. Bohn , C. Bourlieu , F. Carrière , R. Boutrou , M. Corredig , D. Dupont , C. Dufour , L. Egger , M. Golding , S. Karakaya , B. Kirkhus , S. Le Feunteun , U. Lesmes , A. MacIerzanka , A. MacKie , S. Marze , D. J. McClements , O. Ménard , I. Recio , C. N. Santos , R. P. Singh , G. E. Vegarud , M. S. J. Wickham , W. Weitschies and A. Brodkorb , A standardised static in vitro digestion method suitable for food-an international consensus, Food Funct., 2014, 5 , 1113 —1124 RSC .

Y. Wei , Z. Yu , K. Lin , C. Sun , L. Dai , S. Yang , L. Mao , F. Yuan and Y. Gao , Fabrication and characterization of resveratrol loaded zein-propylene glycol alginate-rhamnolipid composite nanoparticles: Physicochemical stability, formation mechanism and in vitro digestion, Food Hydrocolloids, 2019, 95 , 336 —348

A. Mackie and P. Wilde , The role of interactions in defining the structure of mixed protein–surfactant interfaces, Adv. Colloid Interface Sci., 2005, 117 , 3 —13

E. Guzmán , S. Llamas , A. Maestro , L. Fernández-Peña , A. Akanno , R. Miller , F. Ortega and R. G. Rubio , Polymer-surfactant systems in bulk and at fluid interfaces, Adv. Colloid Interface Sci., 2016, 233 , 38 —64

D. J. French , P. Taylor , J. Fowler and P. S. Clegg , Making and breaking bridges in a Pickering emulsion, J. Colloid Interface Sci., 2015, 441 , 30 —38

E. Dickinson Mixed biopolymers at interfaces: Competitive adsorption and multilayer structures, Food Hydrocolloids, 2011, 25 , 1966 —1983

F. Liu , C. Ma , D. J. McClements and Y. Gao , Development of polyphenol-protein-polysaccharide ternary complexes as emulsifiers for nutraceutical emulsions: Impact on formation, stability, and bioaccessibility of β-carotene emulsions, Food Hydrocolloids, 2016, 61 , 578 —588

F. Liu , D. Wang , H. Xu , C. Sun and Y. Gao , Physicochemical properties of β-carotene emulsions stabilized by chlorogenic acid–lactoferrin–glucose/polydextrose conjugates, Food Chem., 2016, 196 , 338 —346

L. Dai , C. Sun , Y. Wei , L. Mao and Y. Gao , Characterization of Pickering emulsion gels stabilized by zein/gum arabic complex colloidal nanoparticles, Food Hydrocolloids, 2018, 74 , 239 —248

L. Bai and D. J. McClements , Formation and stabilization of nanoemulsions using biosurfactants: Rhamnolipids, J. Colloid Interface Sci., 2016, 479 , 71 —79

Y. Wei , C. Sun , L. Dai , L. Mao , F. Yuan and Y. Gao , Novel Bilayer Emulsions Costabilized by Zein Colloidal Particles and Propylene Glycol Alginate, Part 1: Fabrication and Characterization, J. Agric. Food Chem., 2019, 67 , 1197 —1208 R. B. Lovaglio , F. J. dos Santos , M. Jafelicci and J. Contiero , Rhamnolipid emulsifying activity and emulsion stability: pH rules, Colloids Surf., B, 2011, 85 , 301 —305

A. B. Pawar , M. Caggioni , R. Ergun , R. W. Hartel and P. T. Spicer , Arrested coalescence in Pickering emulsions, Soft Matter, 2011, 7 , 7710 —7716 RSC .

Y. Zou , J. Guo , S.-W. Yin , J.-M. Wang and X.-Q. Yang , Pickering Emulsion Gels Prepared by Hydrogen-Bonded Zein/Tannic Acid Complex Colloidal Particles, J. Agric. Food Chem., 2015, 63 , 7405 —7414

E. Dickinson Exploring the frontiers of colloidal behaviour where polymers and particles meet, Food Hydrocolloids, 2016, 52 , 497 —509

A. Sarkar , S. Zhang , M. Holmes and R. Ettelaie , Colloidal aspects of digestion of Pickering emulsions: Experiments and theoretical models of lipid digestion kinetics, Adv. Colloid Interface Sci., 2019, 263 , 195 —211

A. Sarkar , V. Ademuyiwa , S. Stubley , N. H. Esa , F. M. Goycoolea , X. Qin , F. Gonzalez and C. Olvera , Pickering emulsions co-stabilized by composite protein/polysaccharide particle-particle interfaces: Impact on in vitro gastric stability, Food Hydrocolloids, 2018, 84 , 282 —291

O. Torres , B. S. Murray and A. Sarkar , Overcoming in vitro gastric destabilisation of emulsion droplets using emulsion microgel particles for targeted intestinal release of fatty acids, Food Hydrocolloids, 2019, 89 , 523 —533

C. Dima , E. Assadpour , S. Dima and S. M. Jafari , Bioavailability of nutraceuticals: Role of the food matrix, processing conditions, the gastrointestinal tract, and nanodelivery systems, Compr. Rev. Food Sci. Food Saf., 2020, 1 —41

A.-I. Mulet-Cabero , L. Egger , R. Portmann , O. Ménard , S. Marze , M. Minekus , S. Le Feunteun , A. Sarkar , M. M.-L. Grundy , F. Carrière , M. Golding , D. Dupont , I. Recio , A. Brodkorb and A. Mackie , A standardised semi-dynamic in vitro digestion method suitable for food – an international consensus, Food Funct., 2020, 11 , 1702 —1720 RSC .

Q. Guo , A. Ye , N. Bellissimo , H. Singh and D. Rousseau , Modulating fat digestion through food structure design, Prog. Lipid Res., 2017, 68 , 109 —118

J. Maldonado-Valderrama , P. Wilde , A. Macierzanka and A. Mackie , The role of bile salts in digestion, Adv. Colloid Interface Sci., 2011, 165 , 36 —46